THE EUROPEAN
PHYSICAL JOURNAL PLUS

Flow through membrane built up by impermeable spheroid coated with porous layer under the influence of uniform magnetic field: effect of stress jump condition

Pramod Kumar Yadav[1,a] (iD)**, Sneha Jaiswal**[1]**, Jaikanth Yadav Puchakatla**[1]**,**
Manoj Kumar Yadav[2]

[1] Department of Mathematics, Motilal Nehru National Institute of Technology Allahabad, Prayagraj, U.P. 211004, India
[2] Department of Mathematics, Noida Institute of Engineering and Technology, Greater Noida 201306, India

Abstract The present problem is concerned with the axi-symmetrical flow of viscous Newtonian fluid over the membrane composed of spheroidal particles with impermeable core. Here, we analyzed the hydrodynamic permeability of the membrane when the steady, axi-symmetric, Newtonian fluid with uniform velocity $\tilde{U}$ is passing through the membrane along z-axis. The Stokes flow takes place in the presence of transversely applied magnetic field $\tilde{\mathbf{B}}$ of uniform strength. A method named as cell model technique is used to reduce the problem of aggregates of particles into the problem of single particle. On the solid surface, no-slip condition and on the fluid–porous interface, continuity of velocity components & normal stress, discontinuity of shearing stress is employed. On the boundary of enveloping cell, we have employed Happel's model, Kuwabara's model, Kvashnin's model, and Mehta–Morse's model. The comparison of the hydrodynamic permeability and normalized mobility of the particles obtained by all above four well-known boundary conditions at hypothetical cell is shown graphically. In this work, we discussed about the various controlling parameters (fluid parameters) which can be used to control the hydrodynamic permeability of the membrane. Some previous results are also reviewed using the results of present problem and also shown the important comparisons with the former problems.

1 Introduction

1.1 Porous medium and porous membrane

The fluid flow problem through the porous media is one of the important studies, as it has numerous applications. Thousands of works have been done on the modeling of fluid flow through porous media. Such discussed problem by researchers have attracted many environmentalists, engineers, industrialists, doctors and also to the educationist from various disciplines, such as earth sciences, bio- medical, geothermal, geological. It is to be observed that almost all the existing materials are porous to some extent [1]. Concrete, chalks, rye bread, sponge, adsorbents, filters, soil, mud, etc., all are examples of porous medium. Some

[a] e-mail: pramodky@mnnit.ac.in (corresponding author)

Springer

of applications of fluid flow through porous media are blood flow through arteries, crude oil refineries in oil reservoirs, filtration of underground water using filters, transport of food to the plants, our skin, and tissues all of which are dealing with porosity. Every fluid flow problem is governed by some equations and the equations governing the flow past a porous media is given by Darcy [2] in 1856. He found experimentally that for fluid flow through porous medium, the pressure drop is directly proportional to the flow velocity. Later on, it was found that Darcy's law is valid only for the laminar flow and for flow through porous medium of low porosity. Brinkman [3] modified Darcy's law and given the equation for the flow through high-porosity material by adding diffusive term.

Porous membrane is built up by the swarm of particles, and fluid flow through such membranes has lots of industrial applications such as in filtration processes, being used in a wide range for solute separation from the solvent, the desalination of brackish, seawater and the production of pure water, food juice, sugars from sugarcane, in the treatment of wastewater, etc. During the process of filtration, the termination of particles and the adhesion of the chemical species on the surfaces of the solid particles take place. Both the aforementioned processes result in the formation of porous shells in the membrane. The formation of porous shell on the solid particles has direct effect on the hydrodynamics drag force experiences by flowing fluid on the particles. Such type of membrane study is done in our present work.

1.2 Cell model technique

The fluid flow through membrane which is built up by swarm of particle has lots of applications. It is inconvenient to study the fluid flow through each and every particles of the membrane. To avoid such complications, one has to adopt the method in which the whole problem is confined to a single cell.

The cell model method [4] is one which gives answer concerning to the problems of porous membranes. This method implies on the swarm of particles, which converts the analysis of whole problem of flow through porous membrane into the single particle covered in a hypothetical cell. The volume of the hypothetical cell is so chosen that the volume occupied by the solid in cell must be equal to that of the volume occupied by solid in the random assemblage of the porous particles. This method is generally applied to the problems which involve clusters of particles such as grains in a defined space, filters, soils, etc. Based on shape of enveloping cell many researchers studied the flow problems through membranes.

Uchida [5] proposed a cell model in which each particle is enveloped by the cubic cell. Though the cubic structure fulfills the space but the difference in inner and outer structures led to the three-dimensional flow. Keeping this disadvantage in mind, Happel [6] and Kuwabara [7] proposed the model in which both the particles and the envelope have same shape. They developed sphere-in-cell, cylinder-in-cell and spheroid-in-cell models. This formulation leads to the axi-symmetrical flow which has simple analytical solutions. Kuwabara [7] assumed that inner particle is solid and stationary and fluid flows around it with constant velocity, whereas Happel [6] assumed that the enclosed particle is moving with constant velocity. Kvashnin [8], and Mehta–Morse [9] along with Happel [6] and Kuwabara [7] also gave the boundary conditions at the hypothetical cell surface. All above four boundary conditions gave rise to four different cell models, respectively known as Happel's, Kuwabara's, Kvashnin's, and Mehta–Morse's models.

Not every structure is perfect sphere many are somehow deviates from the sphere shape. There are lots of applications and model discussed on the shape of particles, some are presented here. Epstein and Masliyah [10] generalized the sphere-in-cell model by particle-in-cell method for the spheroids. They solved the problem numerically. They faced difficulty

in getting solution of governing equation which was in terms of stream function $E^4\psi = 0$. Dassios et al. [11] later solved this problem by introducing the method of semi separation of variables. In 1995, Dassios et al. [12] studied the Stokes flow problem through the swarms of spheroidal particles. They made use of particle-in-cell method and applied Happel's and Kuwabara's boundary conditions to the problem. They concluded graphically that the Happel's model is superior to that of Kuwabara's model. The study of momentum transfer at the fluid-porous interface was done by Ochoa-Tapia and Whitaker [13]. They developed a new boundary condition regarding the momentum transfer known as stress jump boundary condition. Yadav et al. [14] solved the problem of fluid flow through spherical particles covered with porous cells using the discontinuous momentum transfer condition at the interface of fluid and porous region, respectively. All four models of cell technique were discussed and compared. The drag force on the particles and the permeability of the membrane composed of the spherical particles was also evaluated and verified by the previous work done. The creeping motion of fluid passing through the swarm of porous spheroidal particles using Kuwabara's boundary conditions was discussed by Deo and Gupta [15]. They numerically calculated the drag coefficient and seen the variation with solid volume fraction for different values of the deformation parameter. Apart from spherical-in-cell and spheroidal-in-cell, Yadav [16] worked on cylinder-in-cell model. He studied the fluid flow through the swarm of cylindrical particles and analyzed the drag force on the particles and also evaluated the permeability of the membrane.

The axis symmetrical Stokes flow passing a swarm of prolate spheroidal particles was discussed by Zlatanovski [17] in 1999. He used Brinkman and Stokes equation for the porous and medium-free fluid region, respectively, in the evaluation of the stream function. He also calculated the Eigen values and Eigen functions for the porous region. Yadav and Deo [18] studied about the viscous fluid flow through the deformed porous sphere placed in another porous medium. They discussed the drag force on the particles and the results were represented graphically. Rajasekhar and Amarnath [19] studied about the flow over porous sphere with solid core. The fluid flow in porous region is governed by Darcy's law and Saffman boundary condition [20] for porous surface. Also evaluated drag force and torque using Faxen's law. Further Bhattacharya and Raja Sekhar [21] modified previous work by using Brinkman equation for the porous region. They discussed the variation of different flow parameters for different flows such as 2D irrotational flow, doublet in uniform flow, rotlet and Stokeslet. Vasin and Filippov [22] calculated the permeability of the membrane theoretically and numerically as well. They considered the membrane composed of spherical particles with solid core. Yadav [23] discussed the creeping flow through a non-homogeneous porous medium. In their work, they considered a membrane built up by non-homogeneous porous cylindrical particle. Cell-model technique has been used to solve the problem of fluid flow through swarm of non-homogeneous porous cylindrical particle and applied all Happel's, Kuwabara's, Kvashnin's, and Mehta–Morse's boundary conditions. The results obtained were displayed graphically and compared with each model. Deo [24] extended the work of Datta and Deo [25] by making slight change in boundary conditions for the problem of Stokes flow through porous circular cylindrical particles. Deo et al. gave very useful daily life application in their paper [26]. They considered the model resembling with the colloid particle covered with the porous layers during the process of dissolution and adsorption. They evaluated the hydrodynamic permeability of the membrane composed of cylindrical porous particle with solid core. Grosan et al. [27] discussed about the steady, viscous fluid flow through the permeable sphere enclosed in another porous sphere. They concluded that the non-dimensional value shear stress increases when each porous parameter increases. Saad [28] presented analytical solution for an axi-symmetrical flow of fluid through the spheroidal

particle-in-cell porous membrane by using Brinkman-Stokes governing equations. Madasu and Bucha [29] have solved the problem of flow through porous membrane formed with the permeable spheroidal cells using coupled Darcy–Stokes equation and the method of cell technique. Recently, Daria [30] has considered the flow of non-Newtonian micropolar fluid through the membrane composed of impermeable spherical cells; it aimed to solve the problem through cell-model technique and validated the result experimentally. All above work discussed is clearly representing the use of cell model technique in the filtration process which involves the porous membrane.

1.3 Magneto-hydrodynamics flows

Magneto-hydrodynamics is the branch of science that deals with the hydrodynamics and electromagnetism of a fluid together. Such flows are attracting due to lots of applications in astrophysics planetary magnetic fields, MHD pumps, MHD generators, MHD flow meters, metallurgy (induction furnace and casting of Al and Fe), dispersion (granulation) of metals, MHD flow control (reduction of turbulent drag, free surface control, etc.), Magnetic filtration and separation, etc. Also, the MHD flows through the porous media has lots of application in medical sciences and in industries. Many researchers [31–34] studied the effect of magnetic field on the flow rate and concluded that flow rate decreases with increase in magnetic number, i.e., magnetic field strength. Such influence of uniform magnetic field on the flow rate motivated many researchers to study the effect of magnetic field on the hydrodynamic permeability of the porous medium. Tiwari et al. [35] got motivated by previous work on magnetic field and studied the effect of applied transverse magnetic field on the permeability of the membrane composed of cylindrical particles. All four cell models and the stress jump condition have been employed to see the effect. Similar work has been done by Srivastava et al. [36] and Yadav et al. [37]. They considered the spherical particles without solid core and with solid core, respectively, and seen the effect on the membrane due to applied magnetic field.

The present work is motivated by the application of MHD flows through the membranes made up of particles of shape deviating from sphere. It is very important to see the porous materials with different angles as complexity is rising due to the geometry of particles. The membrane composing of deformed spherical particles with solid core is taken into study. The slow, viscous, incompressible, electrically conducting fluid is allowed to flow through the considered geometry in the presence of applied transverse magnetic field. The cell-model technique is used to study the problem of magnetohydrodynamics through the porous membrane composing of set of impermeable spheroidal particles. The effect of magnetic field, stress jump coefficient, volume fraction, and deformation parameter on the permeability of the membrane for the four well-known cell models is discussed graphically. The effect of various fluid parameters on normalized mobility of the porous particles is also analyzed graphically. The limiting case of the present problem is validated with the previously established results done so far by the various researchers/scientist.

The novelty of this work lies in the analytical solution of the most complex geometry of the pores in the presence of the magnetic field and reducing the present problem into the several other solved problems. The present work aims at to signify the importance of a biological/synthetic material containing tiny pores (known to be porous membrane) of different shapes. Porous membranes with different characteristics are useful for various types of filtration and extraction process involving oil and gases separation. Some of the works [38–40] signified the importance of membrane in gas separation using graphene-based nanoporous membrane. We have focused on the membrane made up of impermeable spheroid particle

cells. The importance and application on flow through membrane of different geometry particles can be easily understood from the work of Rasoulzadeh and Kuchuk [41]. Rasoulzadeh and Kuchuk beautifully explained an application of spheroid particles in the process of formation of vug and fractures. They solved the problem of effective permeability of a porous medium and showed that how the spheroid shaped vug and fractures brings variation in the flow behavior. Chen [42] solved analytically the problem of fluid extraction through prolate spheroid porous setup. He investigated that the flow rate is higher in the case of spheroid-shaped rather than in the cylinder-shaped porous medium, respectively.

2 Formulation and solution of the problem

2.1 Formulation of the problem

The model considered in the present work is the membrane composing of the impermeable spheroidal particles covered with a porous layer.

The steady, viscous, incompressible, axi-symmetric, creeping motion of Newtonian fluid is allowed to pass through the membrane (Fig. 1) with velocity $\tilde{\mathbf{U}}$ uniformly in positive z-direction. The flow takes place in the presence of transverse applied magnetic field $\tilde{\mathbf{B}}$ with uniform strength. For solution of the problem, the particle-in cell method has been used. So, every impermeable spheroidal particle coated with porous layer is covered by a hypothetical cell surface of same shape as shown in Fig. 2.

Let the surface of the spheroid S_I which deviates little in a shape from that of sphere of radius $\tilde{r} = \tilde{a}$ be $\tilde{r} = \tilde{a}(1 + \delta_n G_n(\varsigma))$. It is being assumed that δ_n is so small that its squares and higher orders are neglected, i.e.,

$$\left(\frac{\tilde{r}}{\tilde{a}}\right)^m = 1 + m\,\delta_n G_n(\varsigma), \tag{1}$$

where m is an integer. In given model, the surface of porous region S_P and of hypothetical cell S_H is assumed as $\tilde{r} = \tilde{b}(1 + \delta_n G_n(\varsigma))$ and $\tilde{r} = \tilde{c}(1 + \delta_n G_n(\varsigma))$, respectively, where $\tilde{a} < \tilde{b} < \tilde{c}$. The radius of hypothetical cell is so chosen that the volume occupied by the impermeable spheroid coated with porous layer in the cell equals to that of volume occupied by the impermeable spheroid coated with porous layer in the membrane.
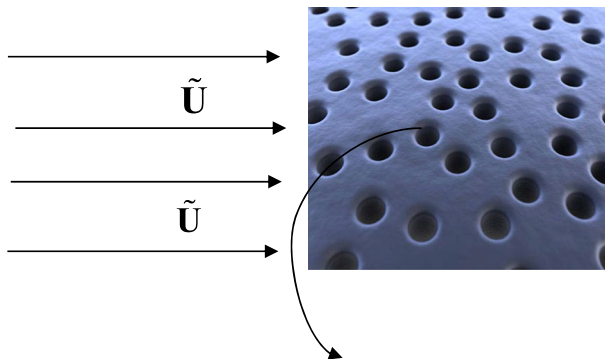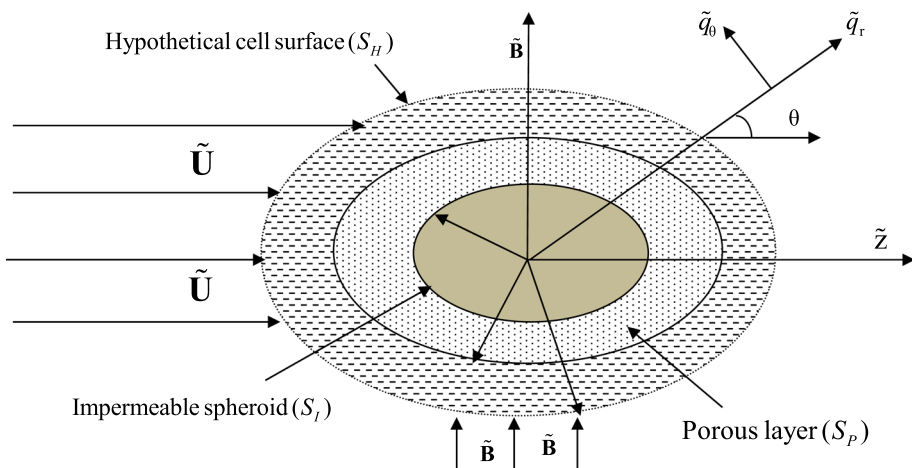

Fig. 1 Physical model of the problem

Fig. 2 Coordinate system of porous spheroid with solid core in a hypothetical cell

2.2 Governing equations

In this work, Stokes equation has been used to study the fluid behavior in the outer fluid envelope while the Brinkman's equation used for the fluid in the porous region. Porous membranes are usually used for filtration process by separating undesirable particles. In filtration process, the fluid that left out of porous are then again re-circulated to filter the fluid more. During this process, the accumulation of fine particles on the pores of the membrane results into the slow creeping flow of the fluid passing through the membrane. Therefore, the process of filtration is fluid flowing at very low Reynolds number, i.e., the convective terms or the inertial terms is completely omitted from the Navier–Stokes equations to model the flow through the membrane. Stokes equation is obtained from the Navier–Stokes Equation by omitting the inertial terms and therefore, it is also known to be creeping motion equation. Stokes equation [4] is given as

$$\tilde{\rho}\frac{\partial \tilde{\mathbf{q}}}{\partial t} = -\tilde{\nabla}\tilde{p} + \tilde{\mu}\,\tilde{\nabla}^2\tilde{\mathbf{q}} + \tilde{\rho}\,\tilde{\mathbf{F}},$$

where $\tilde{\rho}$ and $\tilde{\mu}$ are density and viscosity of flowing fluid with velocity vector $\tilde{\mathbf{q}}$ under the influence of force vector $\tilde{\mathbf{F}}$.

The flow through the porous region can be governed by both the Darcy's and Brinkman's equation where the latter is the modification of the former. Brinkman's equation is widely used for describing the flow in porous medium irrespective of values of permeability and porosity of the porous medium. In 1947, Brinkman [3] had given the following equation for the analysis of the fluid behavior in the porous region:

$$\tilde{\rho}\frac{\partial \tilde{\mathbf{q}}}{\partial t} = -\tilde{\nabla}\tilde{p} + \tilde{\mu}_{\text{eff}}\tilde{\nabla}^2\tilde{\mathbf{q}} - \frac{\tilde{\mu}}{\tilde{k}}\tilde{\mathbf{q}} + \tilde{\rho}\,\tilde{\mathbf{F}}$$

where $\tilde{\mu}_{\text{eff}}$ is an effective viscosity and $\tilde{k}$ is the permeability of the porous medium.

It is difficult to get the general solution of the present problem without accepting any physically consistent assumptions under which the closed form solution of the problem can be obtained. The objective of the work is to find an analytical solution for the present

model and deduce several previous results. For this, authors have considered the following assumption:

1. An incompressible viscous Newtonian fluid flow is axi-symmetric passing through the porous membrane.
2. Flow inside the porous region is governed by the Brinkman model.
3. No external electric field is present and the applied magnetic field is assumed to be so small to produce the valuable induced current.

Because of assumption-3, an electric current density vector $\tilde{\mathbf{J}} = \tilde{\sigma}\,(\tilde{\mathbf{q}} \times \tilde{\mathbf{B}}$, here $\tilde{\sigma}$ is an electrical conductivity of the fluid. Therefore, the direction of the Lorentz force $\tilde{\mathbf{F}} = \tilde{\mathbf{J}} \times \tilde{\mathbf{B}}$ and the velocity $\tilde{\mathbf{q}}$ of fluid is collinear and in opposite directions. We shall denote the regions outside the porous region by superscript 'o' and within the porous region by 'i'.

The governing equation together with continuity condition for the flow outside porous medium is given by Stokes equation as described in the book of Happel and Brenner [4], Jayalakshmamma et al. [43], Srivastava et al. [36]:

$$\tilde{\mu}_h^2\,\tilde{\sigma}^o(\tilde{\mathbf{q}}^o \times \tilde{\mathbf{B}}) \times \tilde{\mathbf{B}} + \tilde{\mu}^o\tilde{\nabla}^2\tilde{\mathbf{q}}^o = \tilde{\nabla}\tilde{p}^o, \quad \tilde{\nabla}\cdot\tilde{\mathbf{q}}^o = 0. \tag{2}$$

The governing equation together with continuity condition for the flow inside the porous region is given by the Brinkman equation (Brinkman [3], Jayalakshmamma et al. [43], Srivastava et al. [36]):

$$-\frac{\tilde{\mu}^o}{\tilde{k}}\tilde{\mathbf{q}}^i + \tilde{\mu}_h^2\,\tilde{\sigma}^i(\tilde{\mathbf{q}}^i \times \tilde{\mathbf{B}}) \times \tilde{\mathbf{B}} + \tilde{\mu}^i\,\tilde{\nabla}^2\tilde{\mathbf{q}}^i = \tilde{\nabla}\tilde{p}^i, \quad \tilde{\nabla}\cdot\tilde{\mathbf{q}}^i = 0. \tag{3}$$

where the symbol ~ denotes the dimensional quantities and $\tilde{\mathbf{q}}^o$, $\tilde{\mathbf{q}}^i$, $\tilde{p}^o$, $\tilde{p}^i$, $\tilde{\mu}^o$, $\tilde{\mu}^i$ are velocities, pressure and viscosity for outer and inner region of the porous spheroid, respectively, $\tilde{\sigma}^o$ and $\tilde{\sigma}^i$ be the electrical conductivity of the fluid for outer and inner region, respectively, $\tilde{k}$ is the permeability of the porous medium & $\tilde{\mu}_h$ is magnetic permeability. Here $\tilde{\mu}^o$ and $\tilde{\mu}^i$ are taken to be different, as according to Liu and Masliyah [44], their relationship depends on the characteristics of the porous medium. The two viscosities $\tilde{\mu}^o$ and $\tilde{\mu}^i$ are equal for the high porosity of the material [45]. The electrical conductivities for both the regions are taken to be equal, i.e., $\tilde{\sigma}^o = \tilde{\sigma}^i = \tilde{\sigma}$.

Taking all the assumptions into consideration, all the above equation reduces to:

$$\tilde{\mu}_h^2\tilde{\sigma}\,(\tilde{\mathbf{q}}^o \times \tilde{\mathbf{B}}) \times \tilde{\mathbf{B}} + \tilde{\mu}^o\tilde{\nabla}^2\tilde{\mathbf{q}}^o = \tilde{\nabla}\tilde{p}^o, \tag{4}$$

$$-\frac{\tilde{\mu}^o}{\tilde{k}}\tilde{\mathbf{q}}^i + \tilde{\mu}_h^2\tilde{\sigma}\,(\tilde{\mathbf{q}}^i \times \tilde{\mathbf{B}}) \times \tilde{\mathbf{B}} + \tilde{\mu}^i\tilde{\nabla}^2\tilde{\mathbf{q}}^i = \tilde{\nabla}\tilde{p}^i, \tag{5}$$

In this problem, the spherical polar coordinate ($\tilde{r}$, $\tilde{\theta}$, $\tilde{\phi}$) is taken where centre of the spheroidal particle represents the origin of coordinate system. As the flow is axi-symmetric, therefore all the fluid parameters will be independent of $\tilde{\phi}$, i.e., $\frac{\partial}{\partial\tilde{\phi}} = 0$ and so the component of velocity $\tilde{q}_{\tilde{\phi}}$ is zero along $\tilde{\phi}$-direction. Here, we assume that the local fluid velocity $\tilde{\mathbf{q}}$ is not perpendicular to magnetic induction vector $\tilde{\mathbf{B}}$, and therefore "in an averaged on its direction," averaged Lorentz's force $(\tilde{\mathbf{q}} \times \tilde{\mathbf{B}}) \times \tilde{\mathbf{B}}$ can be taken as $-0.5\,\tilde{\mathbf{B}}^2\,\tilde{\mathbf{q}}$.

2.3 Solution of the problem

The governing Eqs. (4) and (5) for the flow of fluid outside and inside the impermeable spheroid coated with porous layer can be reduced in non-dimensional form by using the following dimensionless quantities

$$r = \frac{\tilde{r}}{\tilde{b}}, \quad \nabla = \tilde{\nabla} \cdot \tilde{b}, \quad \Delta = \tilde{\Delta} \cdot \tilde{b}^2, \quad p = \frac{\tilde{p}}{\tilde{p}^o},$$

$$\tilde{p}^o = \frac{\tilde{U}\tilde{\mu}^o}{\tilde{b}}, \quad \mathbf{q} = \frac{\tilde{\mathbf{q}}}{\tilde{U}}, \quad \lambda^2 = \frac{\tilde{\mu}^i}{\tilde{\mu}^o}, \quad k = \tilde{k}\tilde{b}^2$$

$$\text{and } \psi^{o.i} = \frac{\tilde{\psi}}{\tilde{U}\,\tilde{b}^2}, \quad \ell = \frac{\tilde{a}}{\tilde{b}}, \quad \frac{1}{\wp} = \frac{\tilde{c}}{\tilde{b}} \tag{6}$$

Thus, the non-dimensional form of governing Eqs. (4) and (5) are:

$$-H^2\mathbf{q}^o + \nabla^2\mathbf{q}^o = \nabla p^o, \quad \nabla \cdot \mathbf{q}^o = 0, \tag{7}$$

$$-\left(\frac{1}{k} + H^2\right)\mathbf{q}^i + \lambda^2\nabla^2\mathbf{q}^i = \nabla p^i, \quad \nabla \cdot \mathbf{q}^i = 0, \tag{8}$$

where $H^2 = \frac{\tilde{\mu}_h^2 \tilde{\sigma} \tilde{B}_o^2 \tilde{b}^2}{2\,\tilde{\mu}^o}$ is the Hartmann number and k is specific permeability of the porous media in dimensionless form and $\tilde{B}_0 = |\tilde{\mathbf{B}}|$ is representing strength of the external magnetic force applied in transverse direction of the flow.

Let us assume that the stream function for outer and inner region of porous media is represented as $\psi^o(r, \theta)$ and $\psi^i(r, \theta)$, respectively. Thus, the velocity components $(q_r, q_\theta, 0)$ in spherical polar coordinates in terms of stream function will be as:

$$q_r^0 = \frac{r^{-2}}{\sin\theta}\frac{\partial\psi^0}{\partial\theta}, \quad q_\theta^0 = -\frac{r^{-1}}{\sin\theta}\frac{\partial\psi^0}{\partial r}, \tag{9}$$

$$q_r^i = \frac{r^{-2}}{\sin\theta}\frac{\partial\psi^i}{\partial\theta}, \quad q_\theta^i = -\frac{r^{-1}}{\sin\theta}\frac{\partial\psi^i}{\partial r}. \tag{10}$$

Using the above expression of velocity's components, the governing Eqs. (7) and (8) will reduce to:

$$E^2(E^2\psi^0 - H^2\psi^0) = o, \tag{11}$$

$$E^2(E^2\psi^i - L^2\psi^i) = o, \tag{12}$$

where $L^2 = \frac{1}{\lambda^2}(H^2 + \frac{1}{k})$ is generalized porosity parameter Srivastava et al. [36] and E^2 is the dimensionless operator given as

$$E^2 = \frac{\partial^2}{\partial r^2} + (1 - \varsigma^2)\frac{\partial^2}{\partial\varsigma^2}, \quad \varsigma = \cos\theta.$$

The remaining quantities such as pressure, shearing stress and normal stress can be obtained by following relations:

$$\frac{\partial p^o}{\partial r} = -\frac{1}{r^2\sin\theta}\frac{\partial}{\partial\theta}(E^2\psi^o) - H^2 q_r^o, \quad \frac{\partial p^0}{\partial\theta} = \frac{1}{\sin\theta}\frac{\partial}{\partial r}(E^2\psi^0) - H^2 q_\theta^0, \tag{13}$$

$$\frac{\partial p^i}{\partial r} = -\frac{\lambda^2 r^{-2}}{\sin\theta}\frac{\partial}{\partial\theta}(E^2\psi^i) - L^2 q_r^i, \quad r^{-1}\frac{\partial p^i}{\partial\theta} = \frac{\lambda^2 r^{-1}}{\sin\theta}\frac{\partial}{\partial r}(E^2\psi^i) - L^2 q_\theta^i; \tag{14}$$

$$\sigma_{r\theta}^o = -p^o + 2\lambda^2\frac{\partial q_r^o}{\partial r}, \quad \sigma_{r\theta}^i = -p^i + 2\lambda^2\frac{\partial q_r^i}{\partial r} \tag{15}$$

$$\sigma_{rr}^o = -p^o + 2\frac{\partial q_r^o}{\partial r}, \quad \sigma_{rr}^i = -p^i + 2\frac{\partial q_r^i}{\partial r} \tag{16}$$

On solving Eqs. (11) and (12) using the method of separation of variables, the stream functions for both the region can be evaluated (Zlatanovski [17]).

$$\psi^o(r,\theta) = \sum_{m=0}^{\infty} \left[\left\{ A_m r^m + B_m r^{1-m} + C_m \sqrt{r} K_\upsilon(H\,r) + D_m \sqrt{r} I_\upsilon(H\,r) \right\} G_m(\varsigma) \right.$$
$$\left. + \left\{ A_m' r^m + B_m' r^{1-m} + C_m' \sqrt{r} K_\upsilon(H\,r) + D_m' \sqrt{r} I_\upsilon(H\,r) \right\} H_m(\varsigma) \right], \tag{17}$$

$$\psi^i(r,\theta) = \sum_{m=0}^{\infty} \left[\left\{ A_m^* r^m + B_m^* r^{1-m} + C_m^* \sqrt{r} K_\upsilon(L\,r) + D_m^* \sqrt{r} I_\upsilon(L\,r) \right\} G_m(\varsigma) \right.$$
$$\left. + \left\{ A_m^{*'} r^m + B_m^{*'} r^{1-m} + C_m^{*'} \sqrt{r} K_\upsilon(L\,r) + D_m^{*'} \sqrt{r} I_\upsilon(L\,r) \right\} H_m(\varsigma) \right] \tag{18}$$

where $I_\upsilon(H\,r)$ & $I_\upsilon(L\,r)$ and $K_\upsilon(H\,r)$ & $K_\upsilon(L\,r)$ are modified Bessel functions of first and second kind, respectively, $\upsilon = m - \frac{1}{2}$, m is an integer and $G_m(\varsigma)$ and $H_m(\varsigma)$ is Gegenbauer function of first and second kind, respectively, of order m and degree $-\frac{1}{2}$. According to expression of Gegenbauer function of second kind, $H_m(\varsigma)$ is infinite along the axis $\varsigma = \pm 1$. Due to this singularity, all primed constants appearing in Eq. (17) and (18) vanishes for all m. Further, in the expression of tangential velocity q_θ in (9) and (10), for $m = 0$ and $m = 1$, it becomes infinite at $\theta = 0$ and $\theta = \pi$. Therefore, after understanding the above facts the final stream function regular solution of both Eqs. (11) and (12) on the axis of symmetry (Zlatanovski [17]) is expressed as follows:

$$\psi^o = [a_2 r^2 + r^{-1} b_2 + K_{\frac{3}{2}}(H\,r) r^{\frac{1}{2}} c_2 + I_{\frac{3}{2}}(H\,r) r^{\frac{1}{2}} d_2]\, G_2(\varsigma)$$
$$+ \sum_m^{\infty} [r^m A_m + r^{1-m} B_m + C_m \sqrt{r} K_\upsilon(Hr) + D_m \sqrt{r} I_\upsilon(H\,r)]\, G_m(\varsigma), \tag{19}$$
$$\psi^i = [a_2^* r^2 + b_2^* r^{-1} + c_2^* \sqrt{r} K_{\frac{3}{2}}(L\,r) + d_2^* I_{\frac{3}{2}}(L\,r)]\, G_2(\varsigma)$$
$$+ \sum_m^{\infty} [r^m A_m^* + r^{1-m} B_m^* + K_\upsilon(L\,r) r^{\frac{1}{2}} C_m^*$$
$$+ I_\upsilon(L\,r) D_m^*]\, G_m(\varsigma), \tag{20}$$

The relation between $G_m(\varsigma)$ and Legendre function $P_m(\varsigma)$ of first kind is given as:

$$G_m(\varsigma) = \frac{P_{m-2}(\varsigma) - P_m(\varsigma)}{2m-1}, \quad m \geq 2$$

In particular,

$$G_2(\varsigma) = \frac{1}{2}(1 - \varsigma^2), \text{ and } G_4(\varsigma) = \frac{1}{8}(1 - \varsigma^2)(5\varsigma^2 - 1).$$

It is important to note that the coefficients a_2, b_2, c_2, d_2, a_2^*, b_2^*, c_2^* and d_2^* contribute to the flow through an impermeable sphere covered with porous layer in spherical shape (Yadav, et al. [37]). This results that all other coefficients in (19) and (20) are of order δ_n. Thus, authors will take surface as a sphere instead of either their exact forms where these coefficients will appear.

2.3.1 Boundary conditions

In order to obtain the solution of concerned problem, i.e., velocity and other physical quantities like pressure, permeability, etc., we need to find the arbitrary constants associated with the stream functions in both the regions. To find these arbitrary constants, we need to define the suitable boundary conditions on the surfaces of the considered model. It is important to note that these boundary conditions should be realistic and valid physically and mathematically.

The appropriate boundary conditions taken for our present problem are discussed below in brief:

1. No-Slip condition at the surface of impermeable spheroid are as:
    Velocity components vanish at the surface of impermeable core, i.e.,

$$q_r^i = 0, q_\theta^i = 0 \text{ at } r = \ell(1 + \delta_n G_n(\varsigma)). \tag{21}$$

2. Continuity of velocity components and normal stress at porous–fluid interface are as:

$$q_r^o = q_r^i, q_\theta^o = q_\theta^i, 2\lambda^2 \frac{\partial q_r^i}{\partial r} - p^i = 2\frac{\partial q_r^0}{\partial r} - p^0 \text{ at } r = (1 + \delta_n G_n(\varsigma)) \tag{22}$$

3. Stress jump boundary condition for shearing stress at $r = (1 + \delta_n G_n(\varsigma))$ given by Ochoa-Tapia and Whitaker [13] be as:

$$\lambda^2 \left(\frac{1}{r} \frac{\partial q_r^i}{\partial \theta} + \frac{\partial q_\theta^i}{\partial r} - \frac{q_\theta^i}{r} \right) - \left(\frac{1}{r} \frac{\partial q_r^o}{\partial \theta} + \frac{\partial q_\theta^o}{\partial r} - \frac{q_\theta^o}{r} \right) = \frac{\beta}{\sqrt{k}} q_\theta^i. \tag{23}$$

4. Continuity of radial the components of flow velocity at hypothetical cell surface $r = \wp^{-1}(1 + \delta_n G_n(\varsigma))$ be as:

$$q_r^o = \cos \theta. \tag{24}$$

On combining all the above seven conditions with any one of the given bellow boundary conditions for enveloping cell models, i.e., Happel's, Kuwabara's, Kvashnin's, and Mehta—Morse's cell models will give the complete solution of the problem:

A. Happel's Model: In this model, Happel [6] suggested that the shearing stress becomes zero at the outer hypothetical cell surface $r = \wp^{-1}(1 + \delta_n G_n(\varsigma))$, i.e.,

$$\sigma_{r\theta}^o(r, \theta) = 0 \text{ or } \frac{\partial^2 \psi^o}{\partial r^2} - 2r^{-1} \frac{\partial \psi^o}{\partial r} - (1 - \varsigma^2) r^{-2} \frac{\partial^2 \psi^o}{\partial \varsigma^2} = o \tag{25}$$

B. Kuwabara's Model: Kuwabara [7] suggest that the vorticity vanishes at hypothetical cell surface $r = \wp^{-1}(1 + \delta_n G_n(\varsigma))$, i.e.,

$$rot(\tilde{\mathbf{q}}^o) = 0 \text{ or } \frac{\partial^2 \psi^0}{\partial r^2} + (1 - \varsigma^2) r^{-2} \frac{\partial^2 \psi^0}{\partial \varsigma^2} = o \tag{26}$$

C. Kvashnin's Model: Kvashnin [8] suggest the symmetry condition on the hypothetical cell surface $r = \wp^{-1}(1 + \delta_n G_n(\varsigma))$, i.e.,

$$\frac{\partial q_\theta^o}{\partial r} = 0. \tag{27}$$

D. Mehta–Morse's Model: Mehta–Morse [9] introduced the homogeneity of the flow on the hypothetical cell surface $r = \wp^{-1}(1 + \delta_n G_n(\varsigma))$, i.e.,

$$q_\theta^o = -\sin \theta. \tag{28}$$

2.3.2 Determination of arbitrary constants

Using the above boundary conditions to the solutions (19)–(20) of the problem along with the following identities:

$$G_n(\varsigma)\,G_2(\varsigma) = -\frac{(n^2 - 5n + 6)}{2(4n^2 - 8n + 3)}G_{n-2}(\varsigma) + \frac{(n^2 - n)}{(4n^2 - 4n - 3)}G_n(\varsigma)$$
$$-\frac{(n^2 + 3n + 2)}{2(4n^2 - 1)}G_{n+2}(\varsigma),$$

$$P_1(\varsigma)G_n(\varsigma)$$
$$= \frac{(n - 2)}{(4n^2 - 8n + 3)}P_{n-3}(\varsigma) + \frac{1}{(4n^2 - 4n - 3)}P_{n-1}(\varsigma) - \frac{(n + 1)}{(4n^2 - 1)}P_{n+1}(\varsigma),$$

we will have eight system of Eqs. (1)–(8) for all the models, which are given in "Appendix A".

As, we already discussed that the leading terms in Eqs. (19) and (20) are responsible for the flow through the impermeable sphere covered with porous layer (Yadav et al. [37]). Hence by solving the systems of Eqs. (9)–(16) given in "Appendix A" for all the models containing only the leading terms, we can obtain the arbitrary constants a_2, b_2, c_2, d_2, a_2^*, b_2^*, c_2^* and d_2^* for all the models.

After getting the values of arbitrary constants a_2, b_2, c_2, d_2, a_2^*, b_2^*, c_2^* and d_2^* for all the models, we used the perturbation method to find all other non-vanishing coefficients A_m, B_m, C_m, D_m, A_m^*, B_m^*, C_m^* and D_m^* appearing in Eqs. (19) and (20) which corresponds to $m = n - 2$, n, $n + 2$ for all the models. Substituting the values of arbitrary constants a_2, b_2, c_2, d_2, a_2^*, b_2^*, c_2^* and d_2^* corresponding to each model in Eqs. (1)–(8) of "Appendix A", we will again obtain system of Eq. (17)–(24) which is placed in "Appendix A".

Thus, explicit expression of the stream functions for the flow through both the regions of impermeable spheroid covered with porous layer will becomes as:

$$\psi^0 = [r^2\,a_2 + r^{-1}\,b_2 + K_{\frac{3}{2}}(H\,r)\,c_2\,r^{\frac{1}{2}} + I_{\frac{3}{2}}(H\,r)\,r^{\frac{1}{2}}\,d_2]\,G_2(\varsigma) + [\,A_{n-2}\,r^{n-2} + B_{n-2}\,r^{-n+3}$$
$$+ C_{n-2}\sqrt{r}\,K_{n-(5/2)}(H\,r) + D_{n-2}\sqrt{r}\,I_{n-(5/2)}(H\,r)]\,G_{n-2}(\varsigma)$$
$$+ [A_n\,r^n + r^{1-n}\,B_n + C_n\,K_{n-\frac{1}{2}}(H\,r)\,r^{\frac{1}{2}}$$
$$+ D_n\,I_{n-\frac{1}{2}}(H\,r)\,r^{\frac{1}{2}}]\,G_n(\varsigma) + [A_{n+2}\,r^{n+2} + B_{n+2}\,r^{-(1+n)} + C_{n+2}\,K_{n+(3/2)}(H\,r)\,r^{\frac{1}{2}}$$
$$+ D_{n+2}I_{n+(3/2)}(H\,r)\,r^{\frac{1}{2}}]\,G_{n+2}(\varsigma),$$

$$(29)$$

$$\psi^i = [a_2^*\,r^2 + b_2^*\,r^{-1} + K_{3/2}(L\,r)\,r^{\frac{1}{2}}\,c_2^* + I_{3/2}(L\,r)\,d_2^*]\,G_2(\varsigma)$$
$$+ [A_{n-2}^*r^{n-2} + B_{n-2}^*\,r^{-n+3} + C_{n-2}^*\,\sqrt{r}\,K_{n-(5/2)}(L\,r) + D_{n-2}^*I_{n-(5/2)}(L\,r)]\,G_{n-2}(\varsigma)$$
$$+ [A_n^*r^n + B_n^*\,r^{-n+1} + C_n^*\,\sqrt{r}K_{n-(1/2)}(L\,r) + D_n^*I_{n-(1/2)}(L\,r)]\,G_n(\varsigma)$$
$$+ [A_{n+2}^*\,r^{n+2} + B_{n+2}^*\,r^{-n-1} + C_{n+2}^*\,\sqrt{r}K_{n+(3/2)}(L\,r) + I_{n+(3/2)}(L\,r)D_{n+2}^*]\,G_{n+2}(\varsigma).$$

$$(30)$$

3 Application to porous oblate spheroid under the influence of magnetic force

In this section, authors considered a membrane which is composed of impermeable oblate spheroid covered with porous layer in oblate spheroidal shape as a particular case of the preceding analysis.

Figure 3 shows the schematic representation of the considered physical model. The equation for the oblate spheroid is given as follows:

$$\frac{x^2 + y^2}{d^2} + \frac{z^2}{d^2(1 - \varepsilon)^2} = 1. \tag{31}$$

here d is an equatorial radius and ε is deformation parameter and it is so small that it's higher powers are neglected.

The polar form of Eq. (31) can be written as $\tilde{r} = \tilde{b}\,(1 + 2\varepsilon\, G_2(\varsigma))$, where $\tilde{b} = \tilde{d}\,(1 - \varepsilon)$. Here it is important to note that for $\varepsilon > 0$, the shape obtained will be of oblate spheroid and for $\varepsilon < 0$, the shape will be of prolate spheroid. This particular case makes our problem a bit easy to obtain the solution. On comparison with the general equation $\tilde{r} = \tilde{b}(1 + \delta_n G_n(\varsigma))$, for the related model we get $n = 2$ and $\delta_n = 2\,\varepsilon$. For $n = 2$, the constants $A_0, B_0, C_0, D_0,$ $A_0^*, B_0^*, C_0^*, D_0^*$ will vanish and the stream functions for the fluid flow through the membrane of oblate spheroids are given by:

$$\psi^o = [a_2\,r^2 + b_2 r^{-1} + K_{3/2}(H\,r)\,r^{\frac{1}{2}}\,c_2 + I_{3/2}(H\,r)\,r^{\frac{1}{2}}\,d_2]\,G_2(\zeta)$$

$$+ [A_2\,r^2 + B_2\,r^{-1} + K_{\frac{3}{2}}(H\,r)r^{\frac{1}{2}}C_2 + I_{3/2}(H\,r)r^{\frac{1}{2}}D_2]\,G_2(\varsigma)$$

$$+ [r^4 A_4 + r^{-3} B_4 + K_{7/2}(H\,r)r^{\frac{1}{2}}C_4 + I_{7/2}(H\,r)r^{\frac{1}{2}}D_4]\,G_4(\varsigma), \tag{32}$$

$$\psi^i = [r^2\,a_2^* + b_2^*\,r^{-1} + K_{\frac{3}{2}}(L\,r)r^{\frac{1}{2}}\,c_2^* + I_{\frac{3}{2}}(L\,r)\,d_2^*]\,G_2(\varsigma)$$
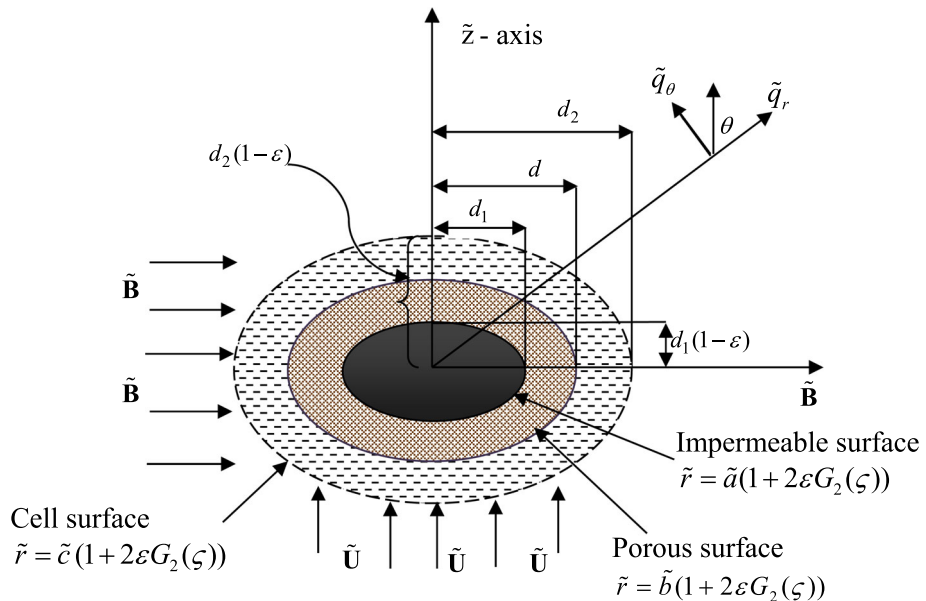

Fig. 3 Coordinate system of oblate spheroid with solid core in a hypothetical cell

$$+ [A_2^* r^2 + B_2^* \, r^{-1} + K_{\frac{3}{2}}(L\,r) r^{\frac{1}{2}} \, C_2^* + I_{\frac{3}{2}}(L\,r) \, D_2^*] \, G_2(\varsigma)$$

$$+ [A_4^* r^4 + B_4^* \, r^{-3} + K_{\frac{7}{2}}(L\,r) \, r^{\frac{1}{2}} \, C_4^* + I_{\frac{7}{2}}(L\,r) r^{\frac{1}{2}} \, D_4^*] \, G_4(\varsigma). \tag{33}$$

4 Evaluation of drag force, normalized particle mobility, and hydrodynamic permeability of the membrane

The membrane filtration has many applications such as in ultra-filtration, nanofiltration, reverse osmosis, and numerous industrial applications. In all aforementioned application, it is very important to find out the hydrodynamic permeability of the porous membrane used. The permeability of membrane depends on the shape of the particles (the membrane composed of), the fluid properties and fluid flow conditions. We aimed in this work to obtain the dragging force exerted on the particles due to the steady flow of incompressible, viscous fluid through the membrane composing of the oblate spheroids and the hydrodynamic permeability of the membrane.

The most important term hydrodynamic permeability of the membrane which is denoted as $\tilde{L}_{11}$ is defined as the ratio of the flow rate $\tilde{U}$ to the cell gradient pressure, i.e., $\frac{\tilde{F}}{\tilde{V}}$.Thus,

$$\tilde{L}_{11} = \frac{\tilde{U}}{\tilde{F}/\tilde{V}}, \tag{34}$$

where $\tilde{V} = \frac{4}{3}\pi \, d_2^2 \, \tilde{c}$ is the volume of the hypothetical cell.

The drag force experienced by each and every particle in presence of magnetic field is given by the formula [3]:

$$\tilde{F} = \pi \, \tilde{\mu}^o \tilde{U} \, \tilde{b} \int\limits_0^\pi \left[\left\{ \varpi^3 \frac{\partial}{\partial r} \left(\frac{E^2 \psi^o}{\varpi^2} \right) \right\} r \right]_{r=1} \mathrm{d}\theta. \tag{35}$$

Here $\varpi = r \sin \theta$ and

$$E^2 \psi^o = \left\{ K_{\frac{3}{2}}(H\,r)H^2 \, r^{\frac{1}{2}} [c_2 + C_2] + I_{\frac{3}{2}}(H\,r) r^{\frac{1}{2}} \, H^2 \, [d_2 + D_2] \right\} G_2(\varsigma)$$

$$+ \left\{ K_{\frac{7}{2}}(H\,r) r^{\frac{1}{2}} H^2 C_4 + I_{\frac{7}{2}}(H\,r) r^{\frac{1}{2}} D_4 H^2 \right\} G_4(\varsigma), \tag{36}$$

Using (36) in (35) and on integration, we obtain the drag force which is given below:

$$\tilde{F} = \pi \, U \tilde{\mu}^o \tilde{b} \, X, \tag{37}$$

where

$$X = \begin{pmatrix} \frac{8}{15}\{H^4 I_{3/2}(H)d_2 + (H^3 + H^4)c_2 K_{1/2}(H)\}\varepsilon + \frac{2}{3}\{(H^3 I_{1/2}(H) - 3H^2 I_{3/2}(H))(d_2 + D_2) \\ + (-3H - 3H^2 - H^3)(c_2 + C_2)K_{1/2}(H)\} \end{pmatrix}. \tag{38}$$

It can be noticed from the expression (37) that only the constants c_2, d_2, C_2 and D_2 contribute to the drag force. Therefore, for each model we can get these constants and hence the drag force on the particles for all four cell models.

From the expression (34) and (37), the hydrodynamic permeability of the membrane can be evaluated. The expression for hydrodynamic permeability of the membrane $\tilde{L}_{11}$ is given as:

$$\tilde{L}_{11} = L_{11} \frac{d_2^2}{\tilde{\mu}^o}, \tag{39}$$

where L_{11} is dimensionless hydrodynamic permeability of the considered membrane and it is expressed as:

$$L_{11} = \frac{4}{3\wp^3 X}, \tag{40}$$

where X is given in Eq. (38).

On substitution of values of constants c_2, d_2, C_2 and D_2 in Eq. (40), we achieved our aim for the concerned problem, i.e., we obtained the hydrodynamic permeability of membrane for all four cell models.

In cell model technique, the setup is done in a manner that the disturbance caused by the neighboring clusters must be confined within the enveloping cell. To analyze this effect, i.e., the hydrodynamic interaction between the inner particle and the surface of the enveloping cell, it is important to discuss about the term "normalized mobility of the particles". Normalized particle mobility (Saad [28], Keh and Cheng [46]) is a dimensionless parameter defined as the ratio between the drag force experienced by the particle in an unbounded medium and the drag force experience under the confinement of the unit cell or enclosure. Mathematically, this term is given as

$$\tilde{M} = \frac{\tilde{F}_{\text{unbouded medium}}}{\tilde{F}_{\text{bouded medium}}}.$$

The drag force in an unbounded medium can be evaluated by taking the limit of X given in Eq. (38) as $\tilde{c} \to \infty$, i.e., $\wp \to 0$ and hence the normalized particle mobility. Clearly, when particle volume fraction $\wp \to 0$ the value of mobility is unity and for $0 < \wp \leq 1$, we have $0 \leq \tilde{M} < 1$. The dependence of normalized mobility of particles on the permeability, volume fraction and on the other flow parameters plays an important role in discussing the various practical applications of the porous membranes in colloidal suspension, flow of blood cells, sedimentation, electrophoresis, agglomeration, etc.

The ratio of drag force $\tilde{F}$ given by (37) and Stokes force $\tilde{F}_S = 6\pi d\,\tilde{\mu}^o \tilde{U}$ is denoted by Ω and is expressed as:

$$\Omega = \frac{(1-\varepsilon)}{6} X. \tag{41}$$

5 Result and discussion

On substitution of constants in Eq. (40) for each discussed model, it is observed that the non-dimensional quantity of hydrodynamic permeability, i.e., L_{11} is the function of $\wp, \beta, k, H, \lambda$ and ε. Thus, the variation of hydrodynamic permeability of membrane is seen with all above parameters graphically. The dependence of fluid flow on the controlling parameters has a significant effect on the analysis of this study. In order to attain the objective of this problem, the numerical values of these controlling parameters which have been used to produce the results are taken from the previously published work, which are discussed below.
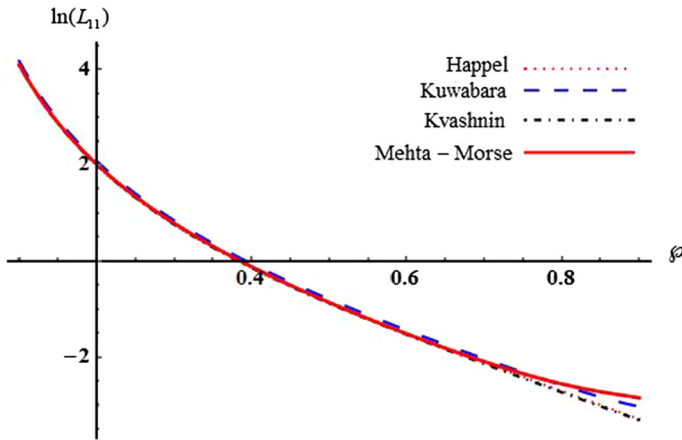
Fig. 4 Variation of $\ln(L_{11})$ of membrane with respect to the volume fraction $\wp$

The volume fraction parameter $\wp = \tilde{b}/\tilde{c}$, which is (volume fraction of particles)$^{1/3}$ and is same as the (volume fraction in the real membrane)$^{1/3}$ ranges between 0 and 1, discussed in the work of Vasin et al. [47]. The stress jump coefficient β takes the value from -1 to 1 which is experimentally proven by Ochoa-Tapia and Whitaker [13, 48] and Kuznetsov [49, 50]. The parameter Hartmann number H always takes the values greater than zero as discussed by the Hartmann and Lazarus [51], Gold [31], Jayalakshmamma [43] and Srivastava et al. [36]. Also, we have considered the values for deformation parameter as $0 < \varepsilon < 1$ and the value of viscosity ratio λ greater than zero.

The effect of particle volume fraction $\wp$ on the non-dimensional hydrodynamic permeability of the membrane is shown in Fig. 4. It is clear from this figure that, as the volume fraction increases the permeability decreases for all the four cell models when other parameters have the values as $H = 3.0$, $\beta = 0.3$, $k = 0.2$, $\lambda = 2.0$, $\ell = 0.5$ and $\varepsilon = 0.3$. This figure illustrates that hydrodynamic permeability of the membrane is maximum when $\wp \to 0$ because under this situation volume of solid phase tends to zero and the model will comprise of no porous shell, therefore the flow will occur with no restrictions. Also, it is noted that flow of all four models is almost coinciding for lower values of $\wp$. This variation of hydrodynamic permeability with the volume fraction is also observed in the works [37, 52, 53] for the membrane built up by spherical particles.

Figure 5 shows the variation of hydrodynamic permeability of membrane with the stress jump coefficient when all other parameters has same values as in previous case and $\wp = 0.8$. While studying the flow through porous media and clear region which involves Brinkman and Stokes equation in the respective regions, one has to consider the Ochoa-Tapia momentum condition because of its significant impact on the physics of the problem [54].

It is seen from Fig. 5 that, as β increases from -1 to 1 the value of hydrodynamic permeability of membrane for all the four cell models increases with it. At $\beta = 0$, the fluid flow through membrane satisfies the continuity of shearing stress. Figure 5 is complete illustration of the hydrodynamic permeability of the membrane for continuous and discontinuous shearing stress at the porous-fluid interface. The increasing order of the hydrodynamic permeability of membrane is as Mehta–Morse $\to$ Kuwabara $\to$ Kvashnin $\to$ Happel, i.e., the hydrodynamic permeability of the membrane is maximum for Happel's cell model and minimum for Mehta–Morse's cell model. Also, it is observed that for positive values β,
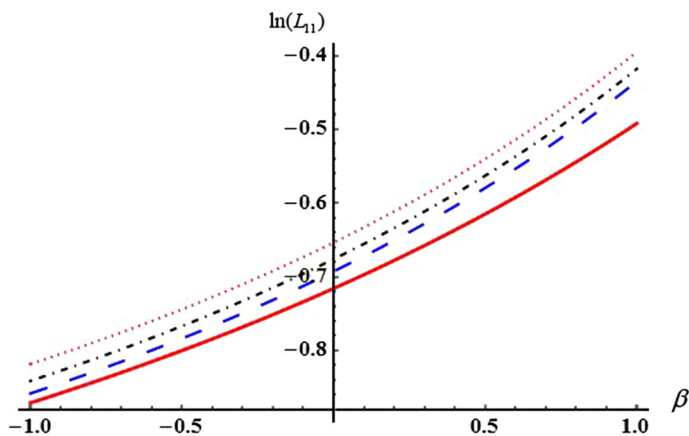
Fig. 5 Variation of $\ln(L_{11})$ of membrane with respect to the stress- jump coefficient β
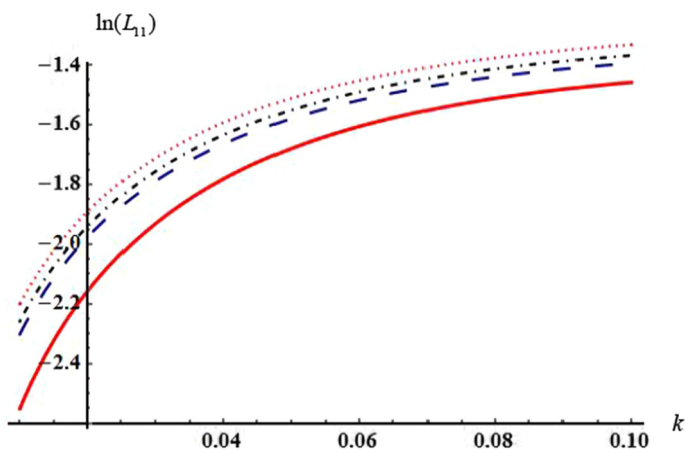

Fig. 6 Variation of $\ln(L_{11})$ of membrane with respect to the specific permeability k

Mehta–Morse's model has much lower value as compare to that of the other's three models. Stress jump coefficient is characteristic of the porous region, it has a direct impact on the hydrodynamic permeability of the membrane and hence cannot be ignored. A similar kind of observation was investigated by Srivastava et al. [36] and Yadav et al. [37] for the problem of hydrodynamic permeability of a membrane built up by porous spherical Particles.

The variation of dimensionless hydrodynamic permeability of the membrane with the specific permeability k of porous region is analyzed by Fig. 6. It can be depicted from the graph that with increase in values of the specific permeability k of porous region, the value of dimensionless hydrodynamic permeability increases for all the four cell models. Similar variation in the natural logarithmic value of hydrodynamic permeability of the porous membrane with the specific permeability of the porous region was observed in the work of Yadav et al. [37]. Permeability defines the characteristic of the porous medium by measuring the ease with which a fluid may pass through the medium (Joseph and Tao [55]) and so it has significant impact on the total permeability of the membrane.
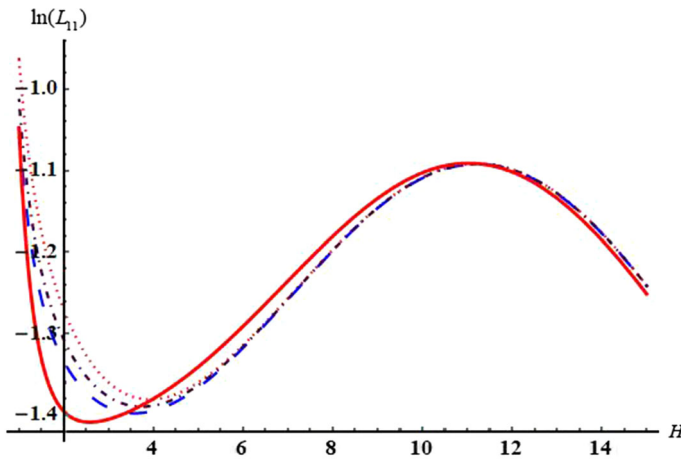
Fig. 7 Variation of $\ln(L_{11})$ of membrane with respect to the Hartmann number H

During the analysis of the result, it is also noticed that the dimensionless hydrodynamic permeability of the membrane increases with increase in values of the specific permeability k till $k < 0.2$ but the nature in variation of hydrodynamic permeability of the membrane with k is reverse when $k > 0.2$. The effect of Hartmann number H on hydrodynamic permeability of the membrane is analyzed by Fig. 7 when $\beta = 0.3$, $k = 0.2$, $\lambda = 2.0$, $\varepsilon = 0.3$, $\wp = 0.8$, and $\ell = 0.5$. Hartmann number is defined for determining the intensity of an external magnetic field. When an electrically conducting fluid passes through the membrane in presence of uniform magnetic field, then a resistive force named as Lorentz force is induced. This Lorentz force is responsible for the variation in the hydrodynamic permeability of a membrane composed by impermeable spheroid coated with porous layer with applied magnetic field.

It can be noticed from Fig. 7 that for all three models; Happel, Kuwabara, Kvashnin, the hydrodynamic permeability of the membrane decreases rapidly with increase in magnetic number H when $H < 3.5$ and $H > 11$. But for Mehta–Morse's model, hydrodynamic permeability of the membrane decreases rapidly with increase in magnetic number H when $H < 2.5$ & $H > 11$. The hydrodynamic permeability of the membrane for Mehta–Morse's and others three models is in increasing nature with magnetic number H when $2.5 < H < 11$ and $3.5 < H < 11$, respectively. For lower values of H the permeability has higher values in which Happel's model has greater value then other. For $H > 5$, Happel, Kuwabara and Kvashnin's models seem to be closer but Mehta–Morse's shows different characteristics. It achieves values greater than other's model for $4 \leq H \leq 11$.

The dependency of hydrodynamic permeability of the membrane on the viscosity ratio λ is discussed through Fig. 8. This figure shows that with increase in viscosity ratio λ, hydrodynamic permeability decreases for all four models. As λ is ratio of viscosity of fluid in porous region to the clear region. Therefore, increase in λ meant increase in viscosity of porous region which decreases the hydrodynamic permeability of the membrane, as expected and also investigated in the work of Vasin et al. [22]. The rate of decrease in hydrodynamic permeability of the membrane when $\lambda < 6$ is faster as compared to the rate of decrease in hydrodynamic permeability of the membrane when $\lambda > 6$. From this figure, we also concluded that the Mehta–Morse's model shows much deviation from the other's three models.

Figure 9 shows the variation of hydrodynamic permeability of the membrane with the deformation parameter ε when $H = 3.0$, $\beta = 0.3$, $k = 0.2$, $\lambda = 2.0$, $\wp = 0.5$, and $\ell = 0.5$. It is clear from the graph that as ε increases, the hydrodynamic permeability of
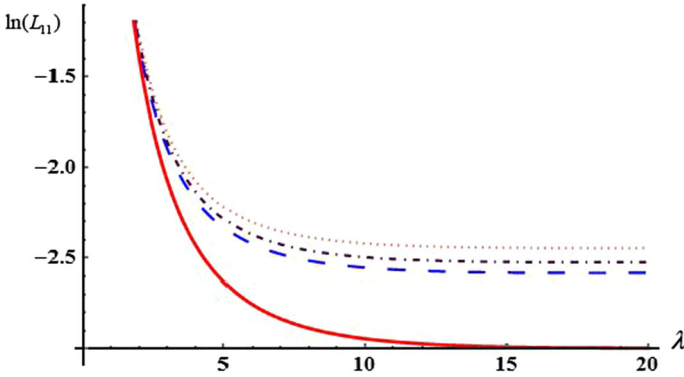
Fig. 8 Variation of $\ln(L_{11})$ of membrane with respect to the viscosity ratio λ
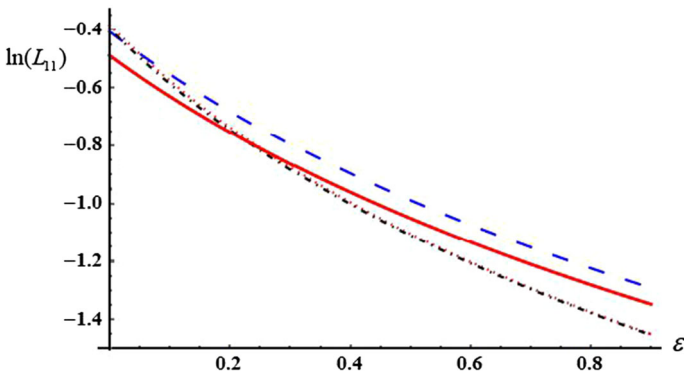

Fig. 9 Variation of $\ln(L_{11})$ of membrane with respect to the deformation parameter ε

the membrane decreases for all four cell models, which validates our result with the work of Yadav et al. [56]. It can be seen from Fig. 9 that for $\varepsilon < 0.2$, Mehta–Morse's model has low value of hydrodynamic permeability as compared to that of other's three cell models. But, for $\varepsilon > 0.2$, Kvashnin's cell model has low values of hydrodynamic permeability as compared to that of other's three cell models.

6 Particular cases

6.1 Stokes flow through a membrane composed by porous spheroid enclosing an impermeable core without magnetic field

When $H \rightarrow 0$, then the above discussed model will reduce to the Stokes flow through a membrane composed by porous spheroid enclosing an impermeable core in absence of magnetic field. In this case, the governing Eqs. (2) and (3), respectively, will reduces as

$$\tilde{\mu}^o \tilde{\nabla}^2 \tilde{\mathbf{q}}^o = \tilde{\nabla} \tilde{p}^o, \quad \tilde{\nabla} \cdot \tilde{\mathbf{q}}^o = 0, \tag{42}$$

$$-\frac{\tilde{\mu}^o}{\tilde{k}} \tilde{\mathbf{q}}^i + \tilde{\mu}^i \, \tilde{\nabla}^2 \tilde{\mathbf{q}}^i = \tilde{\nabla} \tilde{p}^i, \quad \tilde{\nabla} \cdot \tilde{\mathbf{q}}^i = 0. \tag{43}$$
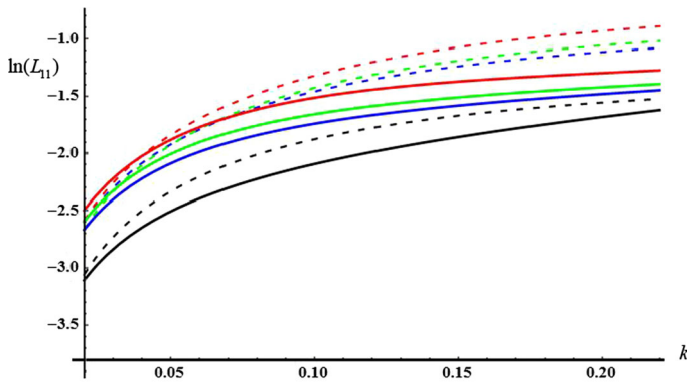
Fig. 10 Comparison in $\ln(L_{11})$ of membrane in presence and absence of magnetic field when $H = 3.0$, $\beta = 0.3$, $\wp = 0.5$, $\lambda = 2.0$, $\varepsilon = 0.05$, and $\ell = 0.5$

The solution of the above equations in terms of stream function will come as:

$$\psi^o(r, \theta) = [a_1 r^2 + \frac{a_2}{r} + a_3 r + a_4 r^4] G_2(\varsigma)$$

$$+ [a_5 r^2 + \frac{1}{r} a_6 + r\, a_7 + r^4\, a_8]\, G_2(\varsigma)$$

$$+ [r^4\, a_9 + r^{-3}\, a_{10} + \frac{1}{r}\, a_{11} + r^6\, a_{12}]\, G_4(\varsigma), \tag{44}$$

$$\psi^i(r, \theta) = [r^2\, b_1 + r^{-1}\, b_2 + K_{\frac{3}{2}}(\eta r)\, r^{\frac{1}{2}}\, b_3 + I_{\frac{3}{2}}(\eta r)\, b_4]\, G_2(\varsigma)$$

$$+ [b_5 r^2 + \frac{1}{r} b_6 + K_{\frac{3}{2}}(\eta r)\, r^{\frac{1}{2}}\, b_7 + I_{\frac{3}{2}}(\eta r) b_8]\, G_2(\varsigma)$$

$$+ [b_9 r^4 + b_{10}\, r^{-3} + b_{11}\, \sqrt{r} K_{\frac{7}{2}}(\eta r) + b_{12} I_{\frac{7}{2}}(\eta r)]\, G_4(\varsigma), \tag{45}$$

where $\eta^2 = \frac{\tilde{\mu}^o}{\tilde{\mu}^i k}$ and $a_i, b_j, i, j = 1, 2, 3, \ldots, 12$ are arbitrary constants and these constants can be obtained by using the boundary conditions (21)–(28) and perturbation method approach.

In this case, the hydrodynamic permeability of the membrane in absence of magnetic field comes out as:

$$L_{11} = \frac{1}{3\,\wp^3} \frac{(1 - \varepsilon)}{\{(1 - \varepsilon)\, a_3 + a_7\}}. \tag{46}$$

The result obtained in this case agrees with the result of Yadav et al. [53].

Figures 10 and 11 show the comparison of dimensionless hydrodynamic permeability of the membrane composed by impermeable spheroid covered with porous layer in oblate spheroidal shape in presence and absence of uniform magnetic field.

Dotted lines and solid lines are used to show the hydrodynamic permeability of membrane in presence and absence of uniform magnetic force, respectively. The models Happle, Kuwabara, Kvashnin's, and Mehta–Morse's are distinguished by red, blue, green and black color, respectively. From Figs. 10 and 11, we concluded that Magnetic field suppressed the hydrodynamic permeability of the membrane when $k < 0.02$ and $\varepsilon < 0.85$ and enhanced the hydrodynamic permeability of the membrane when $k > 0.02$ for all three model except Happel's [Fig. 10]. It enhanced the hydrodynamic permeability of the membrane for Happel's model when $k > 0.05$.
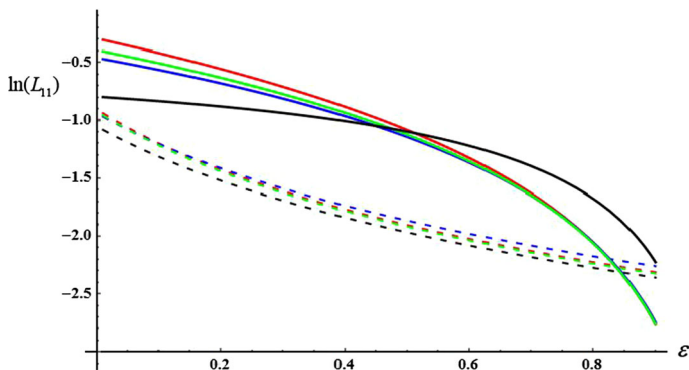
Fig. 11 Comparison in $\ln(L_{11})$ of membrane in presence and absence of magnetic field when $H = 3.0$, $\beta = 0.3$, $\wp = 0.5$, $\lambda = 2.0$, $k = 0.02$, and $\ell = 0.5$

When $\tilde{c} \to \infty$, i.e., $\wp \to 0$, the considered physical model reduces to the impermeable spheroid coated with porous layer in an unbounded medium. In this case, the expressions of non-dimensional form of hydrodynamic drag force is given as

$$\tilde{F} = 4\pi \tilde{\mu}^o d \tilde{U} [(1 - \varepsilon) a_3 + a_7], \tag{47}$$

and the drag force ratio Ω, will comes as:

$$\Omega = \frac{2}{3} [(1 - \varepsilon) a_3 + a_7]. \tag{48}$$

6.2 Stokes flow through a membrane composed by porous oblate spheroid in presence of uniform magnetic field

Under the limiting case $\ell \to 0$, the considered model will reduce to the Stokes flow through a membrane which is composed by porous oblate spheroid in presence of magnetic field. In this case the stream function solution of the governing Eqs. (11) and (12) will be:

$$\psi^o = [a_2 r^2 + r^{-1} b_2 + K_{\frac{3}{2}}(H r) c_2 r^{\frac{1}{2}} + I_{\frac{3}{2}}(H r) d_2 r^{\frac{1}{2}}] G_2(\varsigma)$$

$$+ [A_2 r^2 + \frac{1}{r} B_2 + C_2 K_{\frac{3}{2}}(H r) r^{\frac{1}{2}} + I_{\frac{3}{2}}(H r) D_2 r^{\frac{1}{2}}] G_2(\varsigma)$$

$$+ [A_4 r^4 + B_4 r^{-3} + K_{\frac{7}{2}}(H r) C_4 r^{\frac{1}{2}} + I_{\frac{7}{2}}(H r) D_4 r^{\frac{1}{2}}] G_4(\varsigma), \tag{49}$$

$$\psi^i = [r^2 a_2^* + I_{\frac{3}{2}}(L r) d_2^*] G_2(\varsigma) + [r^2 A_2^* + I_{\frac{3}{2}}(L r) D_2^*] G_2(\varsigma)$$

$$+ [r^4 A_4^* + I_{\frac{7}{2}}(L r) D_4^*] G_4(\varsigma). \tag{50}$$

The hydrodynamic permeability of this kind of membrane is also evaluated by using the formula (34), which comes out as

$$L_{11} = \frac{4}{3\gamma^3 Y}, \tag{51}$$

$$Y = \begin{pmatrix} \frac{8}{15}\{H^4 I_{3/2}(H)d_2 + (H^3 + H^4)c_2 K_{1/2}(H)\}\varepsilon \\ + \frac{2}{3}\{(H^3 I_{1/2}(H) - 3H^2 I_{3/2}(H))(d_2 + D_2) \\ + (-3H - 3H^2 - H^3)(c_2 + C_2)K_{1/2}(H)\} \end{pmatrix}, \tag{52}$$
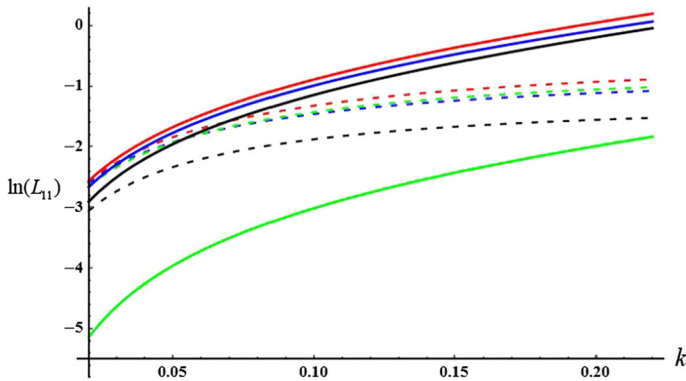
Fig. 12 Comparison in $\ln(L_{11})$ of the membrane composed by porous spheroid and impermeable spheroid covered with porous layer in presence of magnetic field when $H = 3.0$, $\beta = 0.3$, $\wp = 0.5$, $\lambda = 2.0$, $\varepsilon = 0.05$, and $\ell = 0.5$

where the arbitrary constants c_2, d_2, C_2 & D_2 can be obtained by using the suitable boundary conditions (22)–(24) together with one of the cell model boundary condition (25)–(28). This result agrees with the result established by Yadav [52].

The expression for non-dimensional form of hydrodynamic drag force exerted on porous oblate spheroid by an electrically conducting fluid under the condition of external magnetic field in an unbounded medium is given as:

$$\tilde{F} = \frac{2}{15}\pi \, U \tilde{\mu}^o \, d[\{((30H^2 + 4H^4)I_{3/2}(H) - 5H^3 I_{1/2}(H))d_2$$
$$- K_{1/2}(H)(15H + 15H^2 + 3H^3 - 2H^4)c_2\}\varepsilon$$
$$+ 5\{(H^3 I_{1/2}(H) - 3H^2 I_{3/2}(H))(d_2 + D_2)$$
$$+ K_{1/2}(H)(-3H - 3H^2 - H^3)(c_2 + C_2)\}]. \tag{53}$$

The comparative values of hydrodynamic permeability of the membrane composed by porous spheroid and impermeable spheroid covered with porous layer in presence of magnetic field are analyzed through Figs. 12 and 13. The nature of variation in the dimensionless form of hydrodynamic permeability of the membrane composed by porous spheroid under the influence of uniform magnetic field with permeability k and jump coefficient β agrees with the results reported by Yadav [52].

6.3 Stokes flow through a membrane composed by porous oblate spheroid in absence of uniform magnetic field

On taking the limit as $H \to 0$ in the model discussed in Sect. 6.2, the model will reduce to the Stokes flow past a membrane composed by porous oblate spheroid in absence of uniform magnetic field. In this case, the governing equations and its stream function solution and hence the drag force experienced by the membrane and hydrodynamic permeability of the membrane will be as:

$$\tilde{\mu}^o \tilde{\nabla}^2 \tilde{\mathbf{q}}^o = \tilde{\nabla} \tilde{p}^o, \quad \tilde{\nabla}.\tilde{\mathbf{q}}^o = 0, \tag{54}$$

$$-\frac{\tilde{\mu}^o}{\tilde{k}}\tilde{\mathbf{q}}^i + \tilde{\mu}^i \tilde{\nabla}^2 \tilde{\mathbf{q}}^i = \tilde{\nabla} \tilde{p}^i, \quad \tilde{\nabla}.\tilde{\mathbf{q}}^i = 0, \tag{55}$$
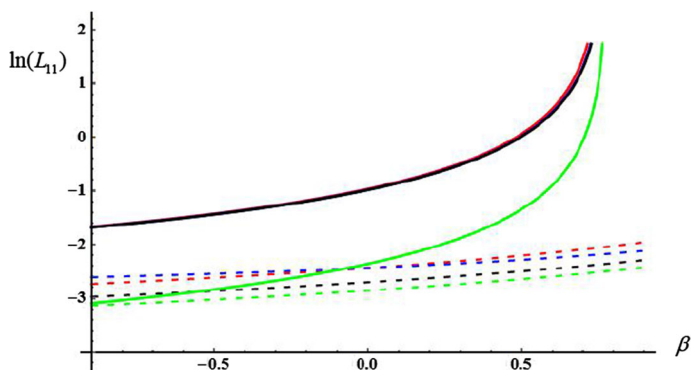
Fig. 13 Comparison in $\ln(L_{11})$ of the membrane composed by porous spheroid and impermeable spheroid covered with porous layer in presence of magnetic field when $H = 3.0, k = 0.2, \wp = 0.8 \; \lambda = 2, \; \varepsilon = 0.05,$ and $\ell = 0.5$

$$\psi^o(r,\theta) = \left[a_1 r^2 + r^{-1} a_2 + a_3 r + a_4 r^4 \right] G_2(\varsigma)$$
$$+ \left[a_5 r^2 + r^{-1} a_6 + r \, a_7 + r^4 \, a_8 \right] G_2(\varsigma)$$
$$+ \left[r^4 \, a_9 + r^{-3} \, a_{10} + r^{-1} \, a_{11} + r^6 \, a_{12} \right] G_4(\varsigma), \tag{56}$$

$$\psi^i(r,\theta) = \left[r^2 b_1 + I_{\frac{3}{2}}(\eta \, r) \, b_2 \right] G_2(\varsigma)$$
$$+ \left[b_3 r^2 + I_{\frac{3}{2}}(\eta \, r) b_4 \right] G_2(\varsigma)$$
$$+ \left[b_5 r^4 + b_6 I_{\frac{7}{2}}(\eta \, r) \right] G_4(\varsigma), \tag{57}$$

$$\tilde{F} = 4 \pi \, \tilde{\mu}^o \, d \, \tilde{U} \left[(1 - \varepsilon) \, a_3 + a_7 \right], \tag{58}$$

$$L_{11} = \frac{1}{3\gamma^3} \frac{(1 - \varepsilon)}{\{(1 - \varepsilon) a_3 + a_7\}}, \tag{59}$$

where $\eta^2 = \frac{\tilde{\mu}^o}{\tilde{\mu}^i k}$ and $a_i, b_j, i = 1, 2, 3, \ldots, 12, j = 1, 2, \ldots, 6$ are arbitrary constants and these constants can be obtained by using the boundary conditions (22)–(24) together with one of the cell model boundary condition (25)–(28).

Under the limiting case $H \to 0$ and $\beta \to 0$, the considered physical problem reduces into the Stokes flow through a membrane composed by porous oblate spheroid in absence of uniform magnetic field and without stress jump condition. The nature of variation in non-dimensional form of hydrodynamic permeability of membrane with different parameters agrees with the work of Yadav et al. [56].

Figures 14 and 15 are presented to show the variation in hydrodynamic permeability of membrane composed by porous spheroid in absence of magnetic field and impermeable spheroid covered with porous layer in presence of magnetic field with permeability k and deformation parameter ε. The nature of variation in the non-dimensional form of hydrodynamic permeability of the membrane composed by porous oblate spheroid with permeability k and deformation parameter ε under the effect of stress jump condition agrees with the variation reported by Yadav [53] which validate our results.

When $\tilde{c} \to \infty$, i.e., $\wp \to 0$ in Eq. (58) then authors obtained the drag force experienced by the porous spheroid in an unbounded medium and hence, for this particular case of the present work, we have also calculated the normalized particle mobility for all four
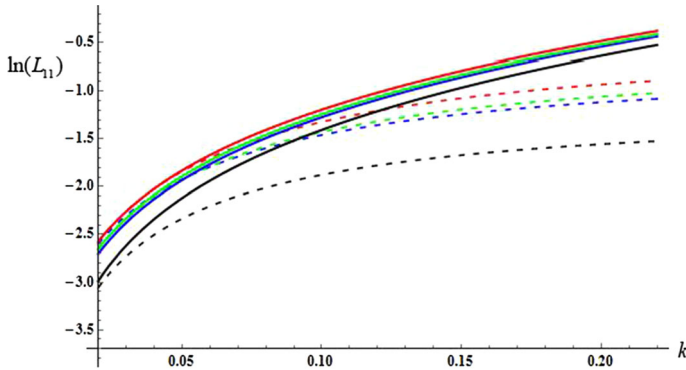
Fig. 14 Comparison in $\ln(L_{11})$ of the membrane composed by porous spheroid in absence of magnetic field and impermeable spheroid covered with porous layer in presence of magnetic field when $H = 3.0, \beta = 0.3, \wp = 0.5, \lambda = 2.0, \varepsilon = 0.05$, and $\ell = 0.5$
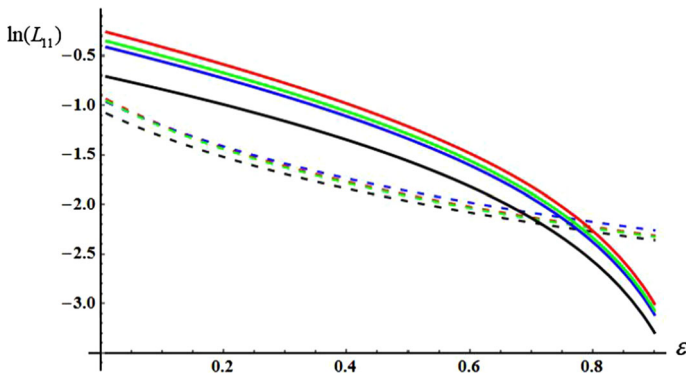

Fig. 15 Comparison in $\ln(L_{11})$ of the membrane composed by porous spheroid in absence of magnetic field and impermeable spheroid covered with porous layer in presence of magnetic field when $H = 3.0, \beta = 0.3, \wp = 0.5, \lambda = 2.0, k = 0.02$, and $\ell = 0.5$

well-known cell models Happel's, Kuwabara's, Kvashnin's, and Mehta–Morse's and have discussed its dependency on various fluid parameters such as particle volume fraction, permeability parameter and stress jump coefficient graphically. Here, we have taken $\lambda = 1$ which yields η to be permeability parameter. Figure 16 reflects the dependence of normalized particle mobility on the permeability parameter η and volume fraction $\wp$ for all four models when $\lambda = 1, \varepsilon = 0.1, \beta = 0.1$. From this figure, it is observed that there is continuous decrease in the mobility of the particles with the increase in the volume fraction of the particles and permeability parameter. For each value of η, mobility is highest for the Happel's model and lowest for the Mehta–Morse's model while other two models are lying in between them.

The nature of variation in the mobility of particle with particle volume fraction $\wp$ and permeability parameter η shown in Fig. 16 agrees with the nature of variation in the mobility of particle with the above parameters in the works carried out by Saad [28], Keh and Cheng [46]. Figure 17 shows the effect of stress jump coefficient β on the particle mobility when $\lambda = 1, \varepsilon = 0.1, \wp = 0.8, \eta = 10$. From Fig. 17, we concluded that the particle mobility can be enhanced/supressed by increasing/decreasing the stress jump coefficient β.
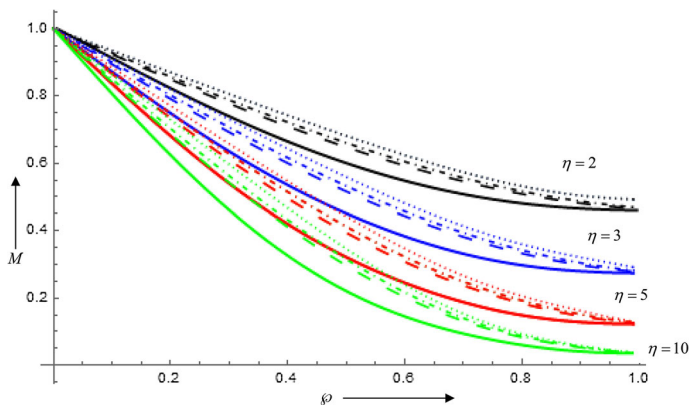
Fig. 16 Variation of mobility of particle M with respect to the particle volume fraction $\wp$ and permeability parameter η
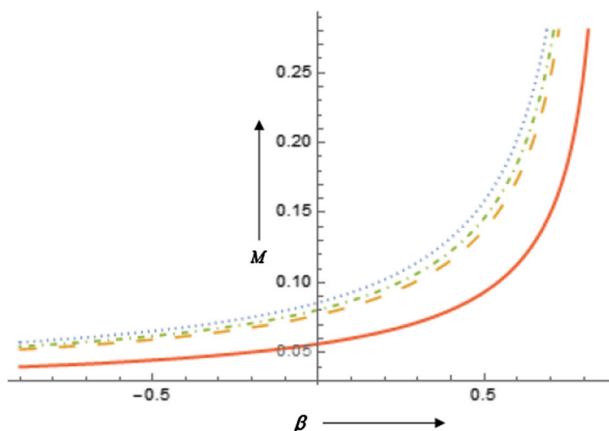

Fig. 17 Variation of mobility of particle M with respect to the stress jump coefficient β

Similar to the previous plot, the mobility of the particles is highest for the Happel's model and lowest for the Mehta–Morse's model. This result clearly shows the importance of discontinuity condition in shearing stress (Stress jump boundary condition) at the fluid porous interface which authors have considered in the present problem. This result has not been discussed in any of the previous aforementioned works.

When $\tilde{c} \to \infty$, i.e., $\wp \to 0$ and $\beta \to 0$ in Eq. (58), then the model will reduces in the model discussed by Saad [28]. In this case, the drag force experienced by the porous spheroid in an unbounded medium comes out as:

$$
\begin{aligned}
\tilde{F} = {}& 12\,\pi\,\tilde{\mu}^o\,d\,\tilde{U}\,\eta^2\lambda^2 [2\,\eta^2\{-5(108 + 18(-12 + \eta^2)\lambda^2 + (108 - 42\,\eta^2 - 5\,\eta^4) \\
& + 4\,\eta^2(6 + \eta^2)\lambda^6) + \varepsilon(-108 + 18\,(12 + 5\,\eta^2)\lambda^2 - 3(36 + 38\,\eta^2 + 3\,\eta^4)\lambda^4 \\
& + 4\,\eta^2(6 + \eta^2)\lambda^6)\}(\eta\,\cosh\eta - \sinh\eta)\sinh\eta + 4\,\eta^4(5(-1 + \lambda^2)\,(-9 - 3(-3 + \eta^2)\,\lambda^2 \\
& + 2\,\eta^2\lambda^4) + \varepsilon\,(9 - 3(6 + \eta^2)\lambda^2 + (9 + 5\,\eta^2 + 2\,\eta^4)\,\lambda^4 - 2\,\eta^2\lambda^6))\,(\sinh\eta)^2 \\
& + (5\,(324 - 648\,\lambda^2 - 3\,(-108 + 24\,\eta^2 + 7\,\eta^4)\lambda^4 + 2\,\eta^2(6 + \eta^2)^2\lambda^6)
\end{aligned}
$$

$$- \varepsilon(-324 + 216(3 + 2\,\eta^2)\lambda^2 + (-324 - 504\,\eta^2 - 27\,\eta^4 + 8\,\eta^6)\lambda^4$$
$$+ 2\,\eta^2(6 + \eta^2)^2\lambda^6))(-\eta\cosh\eta + \sinh\eta)^2)]/5[(54 + 9(-6 + \eta^2)\,\lambda^2$$
$$- 2\,\eta^2(6 + \eta^2)\lambda^4)(\eta\cosh\eta - \sinh\eta) + 2\,\eta^2(-9 - 3(-3 + \eta^2)\lambda^2 + 2\,\eta^2\lambda^4)\sinh\eta]^2$$

It is seen from above expression that when $\eta \to 0$ (*i.e.*, $k \to \infty$) then the mobility of particle is becomes zero because the drag force experienced by the porous spheroid in an unbounded medium becomes zero. This validates our result from the work of the Saad [28].

The porous oblate spheroid becomes solid, when $k \to \infty$. Thus, on taking the limit as $k \to \infty$, in Eq. (59), the non-dimensional form of hydrodynamic permeability of a membrane L_{11H}, L_{11K}, L_{11KV}, and L_{11M} composed by solid spheroid in cell for all Happel, Kuwabara, Kvashnin, and Mehta–Morse cell models, respectively, which has been discussed by Yadav et al. [56] are comes as:

$$L_{11H} = -\frac{5\,(\varepsilon - 1)\,(1 + 2\,\wp + \wp^2)\,(2 + \wp + 2\wp^2)^2\,(\wp - 1)^4}{3\wp^3(3 + 2\wp^5)(10 + 5\,\wp - 5\,\wp^3 - 10\,\wp^4 + (-2 + 5\,\wp + 12\wp^2 + 9\,\wp^3 + 6\,\wp^4)\varepsilon)}, \tag{60}$$

$$L_{11K} = -\frac{2\,(\varepsilon - 1)\,(5 + 6\,\wp + 3\,\wp^2 + \wp^3)^2\,(\wp - 1)^4}{9\wp^3((5 + 6\,\wp + 3\,\wp^2 + \wp^3)\,(5 - 5\wp) + (-5 + 8\,\wp + 21\,\wp^2 + 14\,\wp^3 + 7\wp^4)\varepsilon)}, \tag{61}$$

$$L_{11KV} = -\frac{5\,(-1 + \varepsilon)\,(16 + \wp(21 + \wp(15 + 8\wp)))^2\,(\wp - 1)^4}{18\wp^3(4 + \wp^5)(-5\wp(-5 + \wp(6 + \wp(7 + 8\wp))) - 16(-5 + \varepsilon) + \wp(31 + \wp(78 + \wp(55 + 32\gamma)))\varepsilon)}, \tag{62}$$

$$L_{11M} = -\frac{5(-1 + \wp)^3(4 + \wp(7 + 4\wp))(-1 + \varepsilon)}{18\wp^3(1 + \wp + \wp^2 + \wp^3 + \wp^4)(-5 + \varepsilon)}. \tag{63}$$

The expression for non-dimensional form of hydrodynamic permeability given in Eq. (60)–(63) agrees with the result of Yadav et al. [56].

When $H \to 0, \ell \to 0, k \to \infty$ and $\tilde{c} \to \infty$, i.e., $\wp \to 0$, then the physical model will reduces in solid oblate spheroid in an unbounded medium. Here, the hydrodynamics drag force $\tilde{F}$ exerted on solid oblate spheroid due to flow of non-electrically conducting fluid and drag force ratio Ω are comes out as:

$$\tilde{F} = 6\pi\left(1 - \frac{\varepsilon}{5}\right)\tilde{\mu}^o\,\tilde{U}\,d, \tag{64}$$

$$\Omega = 1 - \frac{\varepsilon}{5}. \tag{65}$$

The expression (64) for the drag force acting on solid oblate spheroid agrees with the result of Palanappan [57], Ramkissoon [54] and Datta and Deo [25] for the flow past a rigid spheroid in an unbounded clear fluid.

6.4 Stokes flow through a membrane composed by porous Sphere with an impermeable core in presence of magnetic field

On taking the limit as $\varepsilon \to 0$, the considered membrane will reduce to the membrane composed by porous sphere enclosing an impermeable sphere.

The hydrodynamic permeability of the membrane built up by porous sphere enclosing an impermeable spherical core will comes as:

$$L_{11} = \frac{4}{2\wp^3\,[\{H^3 I_{1/2}(H) - 3H^2 I_{3/2}(H)\}d_2 + K_{1/2}(H)\{-3H - 3H^2 - H^3\}c_2]}, \tag{66}$$

where c_2 & d_2 are arbitrary constants which is evaluated in Sect. 2.3.2 by solving Eqs. (9)–(15) together with one of the cell model boundary condition (16a)–(16d) given in "Appendix A". The result obtained in this case agrees with the result of Yadav et al. [37].

If $H \to 0$, then the model will reduces to Stokes flow through a membrane of impermeable spherical particle coated with porous layer in spherical shape in absence of magnetic field and this model already has been analyzed by Yadav et al. [14].

6.5 Stokes flow through a membrane composed by porous spherical particle in presence of magnetic field

If $\ell \to 0$, then the model achieved in Sect. 6.4 will reduces in the slow viscous flow of an electrically conducting fluid through the membrane composed by porous spherical particle in presence of uniform magnetic field. In this case, the stream function solution of the concern governing equation will be:

$$\psi^o = [a_2 r^2 + \frac{b_2}{r} + c_2 \sqrt{r}\, K_{3/2}(H\,r) + d_2 \sqrt{r}\, I_{3/2}(H\,r)]\, G_2(\varsigma), \tag{67}$$

$$\psi^i = [a_2^* r^2 + d_2^* I_{3/2}(L\,r)]\, G_2(\zeta). \tag{68}$$

The expression for hydrodynamic permeability of the membrane built up by porous spherical particle which agrees with the expression of hydrodynamic permeability of the membrane given by Yadav [52] comes as

$$L_{11} = \frac{4}{3\wp^3\, Y}, \tag{69}$$

$$Y = \frac{2}{3}[(H^3 I_{1/2}(H) - 3H^2 I_{3/2}(H))d_2 \\ + (-3H - 3H^2 - H^3)\, c_2\, K_{1/2}(H)]. \tag{70}$$

On taking the limit as $H \to 0$, we can find an analytical expression for hydrodynamic permeability of the membrane built up by porous spherical particle in absence of uniform magnetic field when non electrically conducting fluid passing through it.

When, $k \to \infty$, then the membrane will be of solid sphere and the expression for non dimensional form of hydrodynamic permeability of the membrane L_{11H}, L_{11K}, L_{11KV}, and L_{11M} for all models, Happel, Kuwabara, Kvashnin, and Mehta–Morse, respectively, are as:

$$L_{11H} = \frac{2 - 3\wp + 3\wp^5 - 2\wp^6}{6\wp^8 + 9\wp^3}, \tag{71}$$

$$L_{11K} = \frac{-5 + 9\wp - 5\wp^3 - 2\wp^6}{45\wp^3}, \tag{72}$$

$$L_{11KV} = \frac{(1-\wp)^3(16 + 21\wp + 15\wp^2 + 8\wp^3)}{72\wp^3 + 18\wp^8}, \tag{73}$$

$$L_{11M} = \frac{(1-\wp)^3(4 + 7\wp + 4\wp^2)}{18(1 + \wp + \wp^2 + \wp^3 + \wp^4)\wp^3}. \tag{74}$$

The expression (71), (72), (73) and (74) agrees with the expression in given Happel [6], Kuwabara [7], Kvashnin [8], and Mehta–Morse [9], respectively.

On taking the limit as $\wp \to 0$, the problem will become Stokes flow through the solid sphere in an unbounded medium. In this case, the drag force $\tilde{F}$ acting on solid sphere in an unbounded medium when fluid flow takes place through it is:

$$\tilde{F} = 6\pi\,\tilde{\mu}^o\,\tilde{b}\,\tilde{U}. \tag{75}$$

This is a well-known result for the drag force established by Stokes [58] for flow past a solid sphere in an unbounded medium.

7 Conclusions

In present problem, an investigation of hydrodynamic permeability of the porous membrane built up by the spheroidal shaped particles in the presence of transversally applied external magnetic field has been done. An analytical solution of the problem has been discussed in detail through the method of cell model technique. This method introduces four different cell models depending on the boundary conditions taken at the hypothetical enveloping cell of a particle of a porous membrane. All four models have been discussed and compared with each other in the result and discussion section of the manuscript. At the porous–liquid interface, the continuity for normal stresses and continuity of velocity have been used. In addition of the above continuity condition, authors also used a well-known discontinuity condition in the tangential stress at the porous–liquid interface proposed and experimentally verified by Ochoa-Tapia and Whitaker [13, 48] to find the complete solution of the problem. From the above discussion, authors concluded that the discontinuity parameter (jump coefficient) play an important role in controlling of drag force, normalized particle mobility and membrane's hydrodynamic permeability. Hence, the consideration of stress jump coefficient, i.e., discontinuity in shear stress at the fluid-porous interface cannot be ignored.

The variation in the hydrodynamic permeability with the parameters namely, volume fraction, specific permeability, magnetic number, viscosity ratio, deformation parameter and stress jump coefficient are observed in accordance to the physics of the present problem. The nature of variation in the hydrodynamic permeability of the membrane with the afore-mentioned parameters validated with the previous published work on the hydrodynamic permeability of the porous membrane. The most important feature of present problem is that it is reducible to the solutions of almost all previous problems on the hydrodynamic permeability of the porous membrane built up by the spherical or deformed spherical particles, which has been represented in the Sect. 6 of the manuscript. Flow through a membrane built up by porous particles of different shapes are important in natural and technological processes such as the flows through sand beds, petroleum reservoir rocks, in aloxite materials, sedimentation. The result of the present problem provides different ideas for the structuring and modeling of the porous membrane mathematically as well as physically. The analysis made in the present problem has important implications in the filtration processes undergoes in the chemical industries, oil factories, etc.

Appendix A

$$[a_2^* + \ell^{-3}b_2^* + \ell^{-3/2} K_{\frac{3}{2}}(L\,\ell)\,c_2^* + \ell^{-3/2} I_{\frac{3}{2}}(L\,\ell)d_2^*]\,P_1(\varsigma)$$

$$- [3\ell^{-3}\,b_2^* + \ell^{-\frac{3}{2}}(L\,\ell\,K_{1/2}(L\,\ell) + 3K_{\frac{3}{2}}(L\,\ell))\,c_2^*$$

$$- (S\,\ell\,I_{\frac{1}{2}}(L\,\ell) - 3I_{\frac{3}{2}}(L\,\ell))\,\ell^{-\frac{3}{2}}\,d_2^*\,]\,\delta_n\,G_n(\varsigma)\,P_1(\varsigma)$$

$$+ \sum_{m}^{\infty} [\ell^{m-2} A_m^* + \ell^{-m-1} B_m^* + \ell^{-3/2} K_\nu(L\,\ell) C_m^*$$

$$+ \ell^{-3/2} I_\nu(L\,\ell) D_m^*] P_{m-1}(\varsigma) = 0, \tag{1}$$

$$[2a_2^* - \ell^{-3} b_2^* - (L\,\ell^{-\frac{3}{2}} K_{\frac{1}{2}}(L\,\ell) + \ell^{-\frac{3}{2}} K_{\frac{3}{2}}(L\,\ell))c_2^* + (L\,\ell^{-\frac{1}{2}} I_{\frac{1}{2}}(L\,\ell) - \ell^{-\frac{3}{2}} I_{\frac{3}{2}}(L\,\ell))d_2^*]G_2(\varsigma)$$

$$+ [3\,b_2^* \ell^{-3} + \{K_{\frac{1}{2}}(L\,\ell)(L\,\ell^{-1/2} + L^2\ell^{1/2}) + (\ell^{-\frac{1}{2}} L\,K_{\frac{1}{2}}(L\,\ell) + 3\,\ell^{-\frac{3}{2}} K_{\frac{3}{2}}(L\,\ell))\}c_2^*$$

$$+ \{L^2\ell^{\frac{1}{2}} I_{\frac{3}{2}}(L\,\ell) - \ell^{-\frac{3}{2}}(L\,\ell\,I_{\frac{3}{2}}(L\,\ell) - 3I_{\frac{3}{2}}(L\,\ell))\}d_2^*]\delta_n G_n(\varsigma)G_2(\varsigma)$$

$$+ \sum_{m}^{\infty} [m\,\ell^{m-2} A_m^* + \ell^{-(m+1)}(-m+1)B_m^* + \{-\ell^{-1/2} L\,K_{\nu-1}(\ell L) + (-m+1)\ell^{-3/2} K_\nu(\ell L)\}C_m^*$$

$$+ \{\ell^{-1/2} L\,I_{\nu-1}(L\,\ell) + (1-m)\ell^{-3/2} I_\nu(L\,\ell)\}D_m^*]G_m(\varsigma) = 0, \tag{2}$$

$$P_1(\varsigma)\,[a_2 + b_2 + K_{\frac{3}{2}}(H)c_2 + I_{\frac{3}{2}}(H)\,d_2 - a_2^* - b_2^* - K_{\frac{3}{2}}(L)\,c_2^* - I_{\frac{3}{2}}(L)\,d_2^*]$$

$$+ [-3\,b_2 - c_2\{3\,K_{3/2}(H) + H\,K_{\frac{1}{2}}(H)\} + d_2\{H\,I_{\frac{1}{2}}(H) - 3I_{\frac{3}{2}}(H)\}$$

$$+ 3\,b_2^* + c_2^*\{L\,K_{\frac{1}{2}}(L) + 3K_{\frac{3}{2}}(L)\} - d_2^*\{L\,I_{\frac{1}{2}}(L) - 3I_{\frac{3}{2}}(L)\}]\delta_n G_n(\varsigma)P_1(\varsigma)$$

$$+ \sum_{m}^{\infty} [A_m + B_m + C_m K_\nu(H) + D_m I_\nu(H) - A_m^* - B_m^* - C_m^* K_\nu(L)$$

$$- D_m^* I_\nu(L)]P_{m-1}(\varsigma) = 0, \tag{3}$$

$$[2a_2 - b_2 + c_2\{-H\,K_{\frac{1}{2}}(H) - K_{\frac{3}{2}}(H)\} + d_2\{H\,I_{\frac{1}{2}}(H) - I_{\frac{3}{2}}(H)\} - 2a_2^* + b_2^*]$$

$$+ c_2^*\{L\,K_{\frac{1}{2}}(L) + K_{\frac{3}{2}}(L)\} - d_2^*\{L\,I_{\frac{1}{2}}(L) - I_{\frac{3}{2}}(L)\}]G_2(\varsigma)$$

$$+ [3\,b_2 + c_2\{H(H+2)K_{\frac{1}{2}}(H) + 3K_{\frac{3}{2}}(H)\} + d_2\{(H^2+3)I_{\frac{3}{2}}(H) - H\,I_{\frac{1}{2}}(H)\}$$

$$- 3b_2^* - c_2^*\{L(L+2)K_{\frac{1}{2}}(L) + 3K_{\frac{3}{2}}(L)\} - d_2^*\{(L^2+3)I_{\frac{3}{2}}(L) - L\,I_{\frac{1}{2}}(L)\}]\delta_n G_n(\varsigma)G_2(\varsigma)$$

$$+ \sum_{m} m\,A_m + (1-m)B_m + C_m\{-H\,K_{\nu-1}(H) + (1-m)K_\nu(H)\}$$

$$+ D_m\{H\,I_{\nu-1}(H) - (1-m)I_\nu(H)\} - m\,A_m^* - (1-m)B_m^* - C_m^*\{L\,K_{\nu-1}(L) + (1-m)K_\nu(L)\}$$

$$- D_m^*\{L\,I_{\nu-1}(L) + (1-m)I_\nu(L)\}\Big]G_m(\varsigma) = 0 \tag{4}$$

$$[-2H^2 a_2 + (H^2+12)b_2 + c_2\{12K_{\frac{3}{2}}(H) + 4H\,K_{\frac{1}{2}}(H)\} + d_2\{12I_{\frac{3}{2}}(H) - 4H\,I_{\frac{1}{2}}(H)\} + 2\lambda^2 L^2 a_2^*$$

$$- \lambda^2(L^2+12)b_2^* - c_2^*\lambda^2\{12K_{\frac{3}{2}}(L) + 4L\,K_{\frac{1}{2}}(L)\} - d_2^*\lambda^2\{12I_{\frac{3}{2}}(L) - 4L\,I_{\frac{1}{2}}(L)\}]P_1(\varsigma)$$

$$+ [-2H^2 a_2 + (-2H^2 - 48)b_2 + 4c_2\{12K_{\frac{3}{2}}(H) - (5H+H^2)K_{\frac{1}{2}}(H)\} + 4d_2\{-(H^2+12)\,I_{\frac{3}{2}}$$

$$+ 4H\,I_{\frac{1}{2}}(H)\} + 2\lambda^2 L^2 a_2^* + \lambda^2(2L^2+48)b_2^* + 4c_2^*\lambda^2\{12K_{\frac{3}{2}}(L) + (5L+L^2)K_{\frac{1}{2}}(L)\}$$

$$+ 4d_2^*\lambda^2\{(L^2+12)\,I_{\frac{3}{2}}(L) - 4L\,I_{\frac{1}{2}}(L)\}]\delta_n G_n(\varsigma)P_1(\varsigma) + \sum_{m}^{\infty} [-\{m\,H^2 + 2m(m^2 - 3m + 2)\}A_m$$

$$+ \{H^2(-1+m) + 2(m^3 - m)\}B_m + 2\{m(m^2 - 1)K_\nu(H) + m(m-1)H\,K_{\nu-1}(H)\}C_m$$

$$+ 2\{m(m^2 - 1)I_\nu(H) - m(m-1)H\,I_{\nu-1}(H)\}D_m + \lambda^2\{mL^2 + 2m(m^2 - 3m + 2)\}A_m^*$$

$$- \lambda^2\{(m-1)L^2 + 2m(m^2 - 1)\}B_m^* - 2\lambda^2 C_m^*\{m(m^2 - 1)K_\nu(L) + m(m-1)L\,K_{\nu-1}(L)\}$$

$$- 2\lambda^2 D_m^*(m(m^2 - 1)I_\nu(L) - m(m-1)L\,I_{\nu-1}(L))]P_{m-1}(\varsigma) = 0, \tag{5}$$

$$\Big[-6\,b_2 - c_2\{(H^2+6)K_{\frac{3}{2}}(H) + 2H\,K_{\frac{1}{2}}(H)\} - d_2\{(H^2+6)I_{\frac{3}{2}}(H) - 2H\,I_{\frac{1}{2}}(H)\} - 2\frac{\beta}{\sqrt{k}}a_2^*$$

$$+ \left(6 + \frac{\beta}{\sqrt{k}}\right)b_2^* + c_2^* \left\{\lambda^2(L^2+6)\,K_{\frac{3}{2}}(L) + 2\lambda^2 L\,K_{\frac{1}{2}}(L) + \frac{\beta}{\sqrt{k}}(L\,K_{\frac{1}{2}}(L) + K_{\frac{3}{2}}(L))\right\}$$

$$+ d_2^* \left\{(L^2+6)\lambda^2\,I_{\frac{3}{2}}(L) - 2\lambda^2 L\,I_{\frac{1}{2}}(L) - \frac{\beta}{\sqrt{k}}(L\,I_{\frac{1}{2}}(L) - I_{\frac{3}{2}}(L))\right\}\Bigg]G_2(\varsigma)$$

$$- [-24\,b_2 - \{(2H^2+24)K_{\frac{3}{2}}(H) + (H^3 + 2H^2 + 10H)\,K_{\frac{1}{2}}(H)\}\,c_2$$

$$- \{(4H^2+24)\,I_{\frac{3}{2}}(H) - (H^3+8H)\,I_{\frac{1}{2}}(H)\}\,d_2 + \left(24\lambda^2 + 3\frac{\beta}{\sqrt{k}}\right)b_2^*$$

$$\cdot \left\{\lambda^2(2L^2+24)K_{\frac{3}{2}}(L) + \lambda^2(L^3 + 2L^2 + 10L)K_{\frac{1}{2}}(L) + \frac{\beta}{\sqrt{k}}(3K_{\frac{3}{2}}(L) + (L^2+2L)K_{\frac{1}{2}}(L))\right\}c_2^*$$

$$+ \{\lambda^2(4L^2+24)I_{\frac{3}{2}}(L) - \lambda^2(L^3+8L)I_{\frac{1}{2}}(L) + \frac{\beta}{\sqrt{k}}((L^2+3)I_{\frac{3}{2}}(L) - L\,I_{\frac{1}{2}}(L))\}d_2^*]\,\delta_n G_n(\varsigma)G_2(\varsigma)$$

$$+ \sum_{m}^{\infty}[-2m(m-2)A_m - 2(m^2-1)B_m - \{(H^2+2(m^2-1))K_v(H) + 2H\,K_{v-1}(H)\}C_m$$

$$- \{(H^2+2(m^2-1))I_v(H) - 2H\,I_{v-1}(H)\}D_m + \left\{2m(m-2)\lambda^2 - \frac{\beta}{\sqrt{k}}m\right\}A_m^*$$

$$+ \left\{2(m^2-1)\lambda^2 - \frac{\beta}{\sqrt{k}}(1-m)\right\}B_m^* + \{(L^2+2(m^2-1))\lambda^2 K_v(L) - 2L\lambda^2 K_{v-1}(L) - \frac{\beta}{\sqrt{k}}(-L\,K_{v-1}(L)$$

$$+ (1-m)I_v(L))\}C_m^* + \{(L^2+2(m^2-1))\lambda^2 I_v(L) - 2L\lambda^2 I_{v-1}(L) - \frac{\beta}{\sqrt{k}}(L\,I_{v-1}(L)$$

$$+ (1-m)I_v(L))\}D_m^*]\,G_m(\varsigma) = 0, \tag{6}$$

$$[-a_2 - b_2\wp^3 - c_2\,K_{\frac{3}{2}}(H/\wp)\,\wp^{\frac{3}{2}} - d_2\,I_{\frac{3}{2}}(H/\wp)\,\wp^{\frac{3}{2}} + 1]P_1(\varsigma) + [3b_2\wp^3 + c_2\{H\wp^{-1}K_{\frac{1}{2}}(H/\wp)$$

$$+ 3K_{\frac{3}{2}}(H/\wp)\}\wp^{\frac{3}{2}} - d_2\wp^{\frac{3}{2}}\{H\wp^{-1}I_{\frac{1}{2}}(H/\wp) + 3I_{\frac{3}{2}}(H/\wp)\}]\,\delta_n G_n(\varsigma)P_1(\varsigma)$$

$$+ \sum_{m}^{\infty}[A_m\wp^{2-m} + B_m\wp^{m+1} + C_m\wp^{\frac{3}{2}}K_v(H/\wp) + D_m\wp^{\frac{3}{2}}I_v(H/\wp)]P_{m-1}(\varsigma) = 0. \tag{7}$$

Happel's boundary condition:

$$[6\wp^4 b_2 + \{(H^2\wp^{1/2} + 6\wp^{5/2})K_{3/2}(H/\wp) + 2H\wp^{3/2}K_{1/2}(H/\wp)\}c_2 + \{(H^2\wp^{1/2} + 6\wp^{5/2})I_{3/2}(H/\wp)$$

$$- 2H\wp^{3/2}I_{1/2}(H/\wp)\}d_2]G_2(\varsigma) + [-24\wp^4 b_2 - \{(H^3\wp^{-1/2} + 2H^2\wp^{1/2} + 10H\wp^{3/2})K_{1/2}(H/\wp)$$

$$+ (2H^2\wp^{1/2} + 24\wp^{5/2})K_{3/2}(H/\wp)\}c_2 - \{(4H^2\wp^{1/2} + 24\wp^{5/2})I_{3/2}(H/\wp) - (H^3\wp^{-1/2}$$

$$+ 8H\wp^{3/2})I_{1/2}(H/\wp)\}d_2]\,\delta_n G_n(\varsigma)G_2(\varsigma) + \sum_{m}^{\infty}[2m(m-2)\wp^{3-n}A_m + 2(m^2-1)\wp^{m+2}B_m$$

$$+ \{(H^2\wp^{1/2} + 2(m^2-1)\wp^{5/2})K_v(H/\wp) + 2H\wp^{3/2}K_{v-1}(H/\wp)\}C_m$$

$$+ \{(H^2\wp^{1/2} + 2(m^2-1)\wp^{5/2})I_v(H/\wp) - 2H\wp^{3/2}I_{v-1}(H/\wp)\}D_m]G_m(\varsigma) = 0. \tag{8a}$$

Kuwabara's boundary condition:

$$[K_{3/2}(H/\wp)c_2 + I_{3/2}(H/\wp)d_2]G_2(\varsigma) + [-\{(H/\wp)K_{1/2}(H/\wp) + K_{3/2}(H/\wp)\}c_2$$

$$+ \{(H/\wp)I_{1/2}(H/\wp) - I_{3/2}(H/\wp)\}d_2\wp^{3/2}]\delta_n G_n(\varsigma)G_2(\varsigma)$$

$$+ \sum_{m}^{\infty}[C_m K_v(H/\wp) + D_m I_v(H/\wp)]G_m(\varsigma) = 0. \tag{8b}$$

Kvashnin's boundary condition:

$$[3\wp^3 b_2 - \{(3\wp^{5/2} + \wp^{1/2}H^2) + (3\wp^{7/2}H^{-1} + 2\wp^{3/2}H)\}K_{1/2}(H/\wp)c_2$$

$$+ \{(3\wp^{5/2} + H^2\wp^{1/2})I_{3/2}(H/\wp) - HI_{1/2}(H/\wp)\wp^{3/2}\}d_2]G_2(\varsigma) + [-12\wp^4 b_2$$

$$- \{3H^2\wp^{1/2} + 7H\wp^{3/2} + 12H^{-1}\wp^{7/2} + 12\wp^{5/2} + H^3\wp^{-1/2}\}K_{1/2}(H/\wp)c_2$$

$$+ \{(4H\wp^{3/2} + H^3\wp^{-1/2})I_{1/2}(H/\wp) - (3H^2\wp^{1/2} + 12\wp^{5/2})\}d_2] \delta_n$$

$$G_n(\varsigma)\, G_2(\varsigma) + \sum_{m}^{\infty} [m(m-2)\wp^{3-m} A_m + (m^2 - 1)\wp^{m+2} B_m$$

$$+ \{\wp^{5/2}(m^2 - H^2\wp^{-2})K_{v-2}(H/\wp) + (m-1)H^{-1}\wp^{7/2}(2m^2$$

$$- m - 3 + 2H^2\wp^{-2})K_{v-1}(H/\wp)\}C_m + \{\wp^{5/2}(m^2$$

$$- H^2\wp^{-2})I_{v-2}(H/\wp) + (m-1)H^{-1}\wp^{7/2}(2m^2 - m - 3$$

$$+ 2H^2\wp^{-2})I_{v-1}(H/\wp)\}D_m]G_m(\varsigma) = 0. \tag{8c}$$

Mehta–Morse's boundary condition:

$$[2a_2 - \wp^3 b_2 - \{H\, K_{\frac{1}{2}}(H/\wp) + K_{\frac{3}{2}}(H/\wp)\, \wp\}\wp^{\frac{1}{2}} c_2 + \{H\, I_{\frac{1}{2}}(H/\wp)$$

$$- I_{\frac{3}{2}}(H/\wp)\, \wp\}\wp^{\frac{1}{2}} d_2 + 1]\, G_2(\varsigma) + [3\wp^3 b_2 + \{(H\,(H\wp^{-1} + 1)K_{\frac{1}{2}}(H/\wp)\, \wp^{\frac{1}{2}}$$

$$+ (H\wp^{-1}K_{\frac{1}{2}}(H/\wp) + 3K_{\frac{3}{2}}(H/\wp))\, \wp^{\frac{3}{2}}\}c_2 - \{H^2 I_{\frac{3}{2}}(H/\wp)\, \wp^{-\frac{1}{2}}$$

$$- (H\wp^{-1}I_{\frac{1}{2}}(H/\wp) - 3I_{\frac{3}{2}}(H/\wp))\, \wp^{\frac{3}{2}}\}d_2]\, \delta_n\, G_n(\varsigma)G_2(\varsigma)$$

$$+ \sum_{m}^{\infty} [m\, \wp^{2-m} A_m + (1-m)\wp^{m+1} B_m + \{-H\wp^{\frac{1}{2}} K_{v-1}(H/\wp)$$

$$+ (1-m)\, K_v(H/\wp)\, \wp^{\frac{3}{2}}\}C_n + \{H\, I_{v-1}(H/\wp)\, \wp^{\frac{1}{2}}$$

$$+ (1-m)\, I_v(H/\wp)\, \wp^{\frac{3}{2}}\}D_m]\, G_m(\varsigma) = o. \tag{8d}$$

$$a_2^* + \ell^{-3}b_2^* + \ell^{-\frac{3}{2}} K_{\frac{3}{2}}(L\,\ell)c_2^* + \ell^{-\frac{3}{2}} I_{\frac{3}{2}}(L\,\ell)d_2^* = 0, \tag{9}$$

$$2\,a_2^* - \ell^{-3}b_2^* - (L\,\ell^{-\frac{1}{2}} K_{\frac{1}{2}}(L\,\ell) + \ell^{-\frac{3}{2}} K_{\frac{3}{2}}(L\,\ell))c_2^* + (L\,\ell^{-\frac{1}{2}} I_{\frac{1}{2}}(L\,\ell) - \ell^{-\frac{3}{2}} I_{\frac{3}{2}}(L\,\ell))d_2^* = 0, \tag{10}$$

$$a_2 + b_2 + K_{\frac{3}{2}}(H)\, c_2 + I_{\frac{3}{2}}(H)\, d_2 - a_2^* - b_2^* - K_{\frac{3}{2}}(L)\, c_2^* - I_{\frac{3}{2}}(L)\, d_2^* = 0, \tag{11}$$

$$2a_2 - b_2 + c_2\{-H\, K_{\frac{1}{2}}(H) - K_{\frac{3}{2}}(H)\} + d_2\{H\, I_{\frac{1}{2}}(H) - I_{\frac{3}{2}}(H)\}$$

$$- 2\,a_2^* + b_2^* + c_2^*\{L\, K_{\frac{1}{2}}(L) + K_{\frac{3}{2}}(L)\} - d_2^*\{L\, I_{\frac{1}{2}}(L) - I_{\frac{3}{2}}(L)\} = 0, \tag{12}$$

$$- 2H^2 a_2 + (H^2 + 12)\, b_2 + \{12K_{\frac{3}{2}}(H) + 4H\, K_{\frac{1}{2}}(H)\}\, c_2$$

$$+ \{12I_{\frac{3}{2}}(H) - 4H\, I_{\frac{1}{2}}(H)\}\, d_2 + 2L^2\, \lambda^2\, a_2^* - (L^2 + 12)\, \lambda^2 b_2^*$$

$$- \{12K_{\frac{3}{2}}(L) + 4L\, K_{\frac{1}{2}}(L)\}\, \lambda^2\, c_2^* - \lambda^2\{12I_{\frac{3}{2}}(L) - 4L\, I_{\frac{1}{2}}(L)\}\, d_2^* = 0, \tag{13}$$

$$- 6\,b_2 - \{(H^2 + 6)K_{\frac{3}{2}}(H) + 2H\, K_{\frac{1}{2}}(H)\}\, c_2 - d_2\{(H^2 + 6)I_{\frac{3}{2}}(H)$$

$$- 2H\, I_{\frac{1}{2}}(H)\} - 2\frac{\beta}{\sqrt{k}}a_2^* + \left(6 + \frac{\beta}{\sqrt{k}}\right)b_2^* + \{(L^2 + 6)\, \lambda^2\, K_{\frac{3}{2}}(L)$$

$$+ 2\lambda^2 L\, K_{\frac{1}{2}}(L) + \frac{\beta}{\sqrt{k}}(L\, K_{\frac{1}{2}}(L) + K_{\frac{3}{2}}(L))\}\, c_2^* + \{\lambda^2(L^2 + 6)\, I_{\frac{3}{2}}(L)$$

$$- 2\lambda^2 L\, I_{\frac{1}{2}}(L) - \frac{\beta}{\sqrt{k}}(L\, I_{\frac{1}{2}}(L) - I_{\frac{3}{2}}(L))\}\, d_2^* = 0, \tag{14}$$

$$- a_2 - b_2\, \wp^3 - c_2\, K_{\frac{3}{2}}(H/\wp)\, \wp^{\frac{3}{2}} - \wp^{\frac{3}{2}} I_{\frac{3}{2}}(H/\wp)\, d_2 + 1 = 0. \tag{15}$$

Happel's boundary condition

$$6\,\wp^4 b_2 + \{(H^2\,\wp^{\frac{1}{2}} + 6\,\wp^{\frac{5}{2}})K_{\frac{3}{2}}(H/\wp) + 2H\,\wp^{\frac{3}{2}}K_{\frac{1}{2}}(H/\wp)\}\,c_2$$
$$+ \{(H^2\,\wp^{\frac{1}{2}} + 6\,\wp^{\frac{5}{2}})I_{\frac{3}{2}}(H/\wp) - 2H\,\wp^{\frac{3}{2}}I_{\frac{1}{2}}(H/\wp)\}\,d_2 = 0. \tag{16a}$$

Kuwabara's boundary condition:

$$K_{\frac{3}{2}}(H/\wp)c_2 + I_{\frac{3}{2}}(H/\wp)\,d_2 = 0. \tag{16b}$$

Kvashnin's boundary condition:

$$3\wp^3 b_2 - \{\wp^{5/2}(3 + H^2\wp^{-2}) + \wp^{7/2}H^{-1}(3 + 2H^2\wp^{-2})\}K_{1/2}(H/\wp)c_2$$
$$+ \{(3\wp^{5/2} + H^2\wp^{1/2})I_{3/2}(H/\wp) - H\wp^{3/2}I_{1/2}(H/\wp)\}d_2 = 0. \tag{16c}$$

Mehta–Morse's boundary condition:

$$2a_2 - \wp^3 b_2 - \{\wp^{1/2}\,H\,K_{\frac{1}{2}}(H/\wp) + \wp^{\frac{3}{2}}K_{\frac{3}{2}}(H/\wp)\}c_2 + \{H\,\wp^{1/2}\,I_{1/2}(H/\wp) -$$
$$\wp^{3/2}\,I_{3/2}(H/\wp)\}d_2 + 1 = 0. \tag{16d}$$

$$\sum_m^\infty [\ell^{m-2}A_m^* + \ell^{-m-1}B_m^* + \ell^{-3/2}K_\nu(L\,\ell)C_m^* + \ell^{-3/2}I_\nu(L\,\ell)D_m^*]P_{m-1}(\varsigma) = 0, \tag{17}$$

$$\sum_m^\infty [m\,\ell^{m-2}A_m^* + (1-m)\ell^{-m-1}B_m^* + \{-L\,\ell^{-1/2}K_{\nu-1}(L\,\ell) + (1-m)\ell^{-3/2}K_\nu(L\,\ell)\}C_m^*$$
$$+ \{L\,\ell^{-1/2}I_{\nu-1}(L\,\ell) + (1-m)\ell^{-3/2}I_\nu(L\,\ell)\}D_m^*]G_m(\varsigma)$$
$$= p_2\,\delta_n\,[E_{n-2}\,G_{n-2}(\varsigma) + E_n\,G_n(\varsigma) + E_{n+2}\,G_{n+2}(\varsigma)], \tag{18}$$

$$\sum_m^\infty [A_m + B_m + C_m K_\nu(H) + D_m I_\nu(H) - A_m^* - B_m^* - C_m^* K_\nu(L) - D_m^* I_\nu(L)]P_{m-1}(\varsigma) = 0, \tag{19}$$

$$\sum_m [m\,A_m + (1-m)B_m + C_m\{-H\,K_{\nu-1}(H) + (1-m)K_\nu(H)\} + D_m\{H\,I_{\nu-1}(H) - (1-m)I_\nu(H)\}$$
$$- m\,A_m^* - (1-m)B_m^* - C_m^*\{L\,K_{\nu-1}(L) + (-m+1)K_\nu(L)\} - D_m^*\{L\,I_{\nu-1}(L)$$
$$+ (-m+1)\,I_\nu(L)\}]\,G_m(\varsigma) = q_2\,\delta_n\,[E_{n-2}\,G_{n-2}(\varsigma) + E_n\,G_n(\varsigma) + E_{n+2}\,G_{n+2}(\varsigma)], \tag{20}$$

$$\sum_m^\infty [-\{m\,H^2 + 2(m^3 - 3m^2 + 2m)\}A_m + \{(m-1)H^2 + 2(m^3 - m)\}B_m + 2\{(m^3 - m)K_\nu(H)$$
$$+ (m^2 - m)H\,K_{\nu-1}(H)\}C_m + 2\{(m^3 - m)I_\nu(H) - H\,(m^2 - m)\,I_{\nu-1}(H)\}D_m + \lambda^2\{m\,L^2$$
$$+ 2(m^3 - 3m^2 + 2m)\}A_m^* - \lambda^2\{(m-1)L^2 + 2m(m^2 - 1)\}B_m^* - 2\lambda^2 C_m^*\{m(m^2 - 1)K_\nu(L)$$
$$+ (m^2 - m)L\,K_{\nu-1}(L)\} - 2\,\lambda^2 D_m^*(m(m^2 - 1)I_\nu(L) - m(m-1)L\,I_{\nu-1}(L))]P_{m-1}(\varsigma)$$
$$= s_2\,\delta_n\,[T_{n-2}\,P_{n-3}(\varsigma) + T_n\,P_{n-1}(\varsigma) + T_{n+2}\,P_{n+1}(\varsigma)], \tag{21}$$

$$\sum_m^\infty [-2m(m-2)A_m - 2(m^2 - 1)B_m - \{(H^2 + 2(m^2 - 1))K_\nu(H) + 2H\,K_{\nu-1}(H)\}C_m$$
$$- \{(H^2 + 2(m^2 - 1))\,I_\nu(H) - 2H\,I_{\nu-1}(H)\}D_m + \left\{2m(m-2)\lambda^2 - \frac{\beta}{\sqrt{k}}m\right\}A_m^*$$
$$+ \{2(m^2 - 1)\lambda^2 - \frac{\beta}{\sqrt{k}}(1-m)\}B_m^* + \{(L^2 + 2(m^2 - 1))\lambda^2 K_\nu(L) - 2\,L\lambda^2 K_{\nu-1}(L)$$
$$- \frac{\beta}{\sqrt{k}}(-L\,K_{\nu-1}(L) + (1-m)\,I_\nu(L))\}C_m^* + \{(L^2 + 2(m^2 - 1))\lambda^2 I_\nu(L) - 2L\lambda^2 I_{\nu-1}(L)$$

$$- \frac{\beta}{\sqrt{k}}(L\, I_{v-1}(L) + (1-m)I_v(L))\} \, D_m^*] \, G_m(\varsigma) = t_2 \, \delta_n \, [E_{n-2} \, G_{n-2}(\varsigma) + E_n \, G_n(\varsigma) + E_{n+2} \, G_{n+2}(\varsigma)], \tag{22}$$

$$\sum_m^\infty [\wp^{-m+2} A_m + \wp^{1+m} B_m + C_m \wp^{3/2} K_v(H/\wp) + D_m \, \wp^{3/2} I_v(H/\wp)]P_{m-1}(\varsigma)$$

$$= u_2 \, \delta_n \, [T_{n-2} \, P_{n-3}(\varsigma) + T_n \, P_{n-1}(\varsigma) + T_{n+2} \, P_{n+1}(\varsigma)]. \tag{23}$$

Happel's boundary condition:

$$\sum_m^\infty [2m(m-2)\wp^{3-m} A_m + 2(m^2-1)\wp^{m+2} B_m + \{(H^2 \wp^{1/2} + 2(m^2-1)\wp^{5/2})K_v(H/\wp)$$

$$+ 2H\wp^{3/2}K_{v-1}(H/\wp)\}C_m + \{(H^2 \wp^{1/2} + 2(m^2-1)\wp^{5/2})I_v(H/\wp)$$

$$- 2H\wp^{3/2}I_{v-1}(H/\wp)\}D_m]G_m(\varsigma) = w_{21} \, \delta_n \, [E_{n-2}G_{n-2}(\varsigma) + E_n G_n(\varsigma)$$

$$+ E_{n+2} \, G_{n+2}(\varsigma)]. \tag{24a}$$

Kuwabara's boundary condition:

$$\sum_m^\infty [C_m K_v(H/\wp) + D_m I_v(H/\wp)]G_m(\varsigma) = w_{22} \, \delta_n \, [E_{n-2} \, G_{n-2}(\varsigma) + E_n \, G_n(\varsigma) + E_{n+2} \, G_{n+2}(\varsigma)]. \tag{24b}$$

Kvashnin's boundary condition:

$$\sum_m^\infty [m(m-2)\wp^{3-m} A_m + (m^2-1)\wp^{m+2} B_m + \{\wp^{5/2}(m^2 - H^2 \wp^{-2})K_{v-2}(H/\wp)$$

$$+ (m-1)H^{-1}\wp^{7/2}(2m^2 - m - 3 + 2H^2 \wp^{-2})K_{v-1}(H/\wp)\}C_m$$

$$+ \{\wp^{5/2}(m^2 - H^2 \wp^{-2})I_{v-2}(H/\wp) + (m-1)H^{-1}\wp^{7/2}(2m^2 - m - 3$$

$$+ 2H^2 \wp^{-2})I_{v-1}(H/\wp)\}D_m]G_m(\varsigma) = w_{23} \, \delta_n \, [E_{n-2} \, G_{n-2}(\varsigma)$$

$$+ E_n \, G_n(\varsigma) + E_{n+2}G_{n+2}(\varsigma)]. \tag{24c}$$

Mehta–Morse's boundary condition:

$$\sum_m^\infty [m\wp^{2-m} A_m + (1-m)\wp^{m+1} B_m + \{-H\wp^{1/2}K_{v-1}(H/\wp)$$

$$+ (1-m)\wp^{3/2}K_v(H/\wp)\}C_m + \{H\wp^{1/2}I_{v-1}(H/\wp)$$

$$+ (1-m)\wp^{3/2}I_v(H/\wp)\}D_m]G_m(\varsigma) = w_{24} \, \delta_n \, [E_{n-2} \, G_{n-2}(\varsigma)$$

$$+ E_n \, G_n(\varsigma) + E_{n+2} \, G_{n+2}(\varsigma)]. \tag{24d}$$

where

$$p_2 = -L\,\ell^{-1/2}(L\,\ell+1)K_{1/2}(L\,\ell)\,c_2^* - L^2\ell^{1/2}I_{3/2}(L\,\ell)d_2^*,$$

$$q_2 = -(H^2+H)K_{1/2}(H)\,c_2 - H^2 I_{3/2}(H)\,d_2 + (L^2+L)\,K_{1/2}(L)\,c_2^* - L^2 I_{3/2}(L)\,d_2^*,$$

$$s_2 = [(3H^2+60)b_2 + 4\,c_2\{15K_{3/2}(H) + (60+H^2)K_{1/2}(H)\} + 4\,d_2\{-(H^2+15)\,I_{3/2}(H)$$

$$+ 5HI_{1/2}(H)\} - \lambda^2(3L^2+60)b_2^* - 4\,c_2^*\lambda^2\{15K_{3/2}(L) + (60+L^2)K_{1/2}(L)\}$$

$$- 4\,d_2^*\lambda^2\{-(L^2+15)I_{3/2}(L) + 5\,L\,I_{1/2}(L)\}],$$

$$t_2 = \frac{8\beta}{\sqrt{k}}a_2^* - \frac{\beta}{\sqrt{k}}b_2^* + c_2^*\{L^3\lambda^2 K_{1/2}(L) + \frac{\beta}{\sqrt{k}}((L^2-2L)\,K_{1/2}(L) - K_{3/2}(L))\}$$

$$+ d_2^* \{ -\lambda^2 L^3 I_{1/2}(L) + \frac{\beta}{\sqrt{k}} (3 L I_{1/2}(L) + (L^2 - 1)I_{3/2}(L)) \} - H^3 K_{1/2}(H) c_2$$

$$+ H^3 I_{1/2}(H) d_2,$$

$$u_2 = -3a_2 + H \wp^{1/2} K_{1/2}(H/\wp) c_2 - H \wp^{1/2} I_{1/2}(H/\wp) d_2 - 3,$$

$$w_{21} = H^3 \wp^{-1/2} K_{1/2}(H/\wp) c_2 - H^3 \wp^{-1/2} I_{1/2}(H/\wp) d_2,$$

$$w_{22} = H \wp^{-1} K_{1/2}(H/\wp) c_2 - H \wp^{-1} I_{1/2}(H/\wp) d_2,$$

$$w_{23} = \{ H^3 \wp^{-1/2} - H^2 \wp^{1/2} - H \wp^{3/2} \} K_{1/2}(H/\wp) c_2$$
$$- \{ H^2 \wp^{1/2} I_{3/2}(H/\wp) + H^3 \wp^{-1/2} I_{1/2}(H/\wp) \} d_2,$$

$$w_{24} = 3 a_2 - H \wp^{1/2}(2 + H/\wp) K_{1/2}(H/\wp) c_2$$
$$- \{ H^2 \wp^{-1/2} I_{3/2}(H/\wp) - H \wp^{1/2} I_{1/2}(H/\wp) \} d_2,$$

$$E_{n-2} = -\frac{n-3}{2} T_{n-2}, \ E_n = n(n-1)T_n, \ E_{n+2} = \frac{n+2}{2} T_{n+2}$$

$$T_{n-2} = \frac{n-2}{(4n^2 - 8n + 3)}, \ T_n = \frac{1}{(4n^2 - 4n - 3)}, \ T_{n+2} = -\frac{1+n}{(4n^2 - 1)}$$

References

1. F.A. Coutelieris, J.M.P.Q. Delgado, *Transport Processes in Porous Media* (Springer, Berlin, 2012)
2. H.P.G. Darcy, *Les fontaines publiques de la ville de Dijon Paris* (Victor Dalmont, Paris, 1856)
3. H.C. Brinkman, J. Appl. Sci. Res. **A1**, 27–34 (1947)
4. J. Happel, H. Brenner, *Low Reynold Number Hydrodynamics. Martinus Nijoff* (The Hague, Netherlands, 1983)
5. S. Uchida, Int. Sci. Technol.Univ. (transl. by T. Motai) Abstract. Ind. Eng. Chem. **46**, 1194–1195 (1954)
6. J. Happel, A.I.Ch.E. **4**(2), 197–201 (1958)
7. S. Kuwabara, J. Phys. Soc. Jpn. **14**, 527–532 (1959)
8. A.G. Kvashnin, Fluid Dyn. **14**(4), 598–602 (1980)
9. G.D. Mehta, T.F. Morse, J. Chem. Phys. **63**(5), 1878–1889 (1975)
10. N. Epstein, J.H. Masliyah, Chem. Eng. J. **3**, 169–175 (1972)
11. G. Dassios, M. Hadjinicolaou, A.C. Payatakes, Q. Appl. Math. **52**(1), 157–191 (1994)
12. G. Dassios, M. Hadjinicolaou, F.A. Coutelieris, A.C. Payatakes, Int. J. Eng. Sci. **33**(10), 1465–1490 (1995)
13. J.A. Ochoa-Tapia, S. Whitaker, Int. J. Heat Mass Transf. **38**(14), 2635–2646 (1995)
14. P.K. Yadav, A. Tiwari, S. Deo, A. Filippov, S. Vasin, Acta Mech. **215**(1–4), 193–209 (2010)
15. S. Deo, B.R. Gupta, Acta Mech. **203**(3–4), 241–254 (2008)
16. P.K. Yadav, Meccanica **48**(7), 1607–1622 (2013)
17. T. Zlatanovski, Q. J. Mech. Appl. Math. **52**(1), 111–126 (1999)
18. P.K. Yadav, S. Deo, Meccanica **47**(6), 1499–1516 (2012)
19. G.P.R. Sekhar, T. Amaranath, Mech. Res. Commun. **23**(5), 449–460 (1996)
20. P.G. Saffman, Stud. Appl. Math. **50**(2), 93–101 (1971)
21. A. Bhattacharyya, G.P. Raja Sekhar, Z. Angew, Math. Phys. **56**(3), 475–496 (2005)
22. S.I. Vasin, A.N. Filippov, Colloid J. **66**(3), 266–270 (2004)
23. P.K. Yadav, Eur. Phys. J. Plus **133**, 1 (2018)
24. S. Deo, Sadhana **29**(4), 381–387 (2004)
25. S. Datta, S. Deo, Proc. Indian Acad. Sci. (Math. Sci.) **112**(3), 463–475 (2002)
26. S. Deo, A. Filippov, A. Tiwari, S. Vasin, V. Starov, Adv. Colloid Interface Sci. **164**(1–2), 21–37 (2011)
27. T. Grosan, A. Postelnicu, I. Pop, Transp. Porous Med. **81**(1), 89–103 (2009)
28. EI Saad. J. Porous Media, 15(9), (2012)
29. K.P. Madasu, T. Bucha, Int. J. Appl. Comput. Math. **5**(4), 109 (2019)
30. D. Khanukaeva, Theor. Comput. Fluid Dyn. **34**(3), 215–229 (2020)
31. R.R. Gold, J. Fluid Mech. **13**(04), 505–512 (1962)

32. S. Globe, Phys. Fluids **2**(4), 404–407 (1959)
33. R. Bali, U. Awasthi, Appl. Math. Comput. **188**(2), 1635–1641 (2007)
34. P.K. Yadav, S. Jaiswal, T. Asim, R. Mishra, Eur. Phys. J. Plus **133**, 247 (2018)
35. A. Tiwari, S. Deo, A. Filippov, Colloid J. **74**(4), 515–522 (2012)
36. B.G. Srivastava, P.K. Yadav, S. Deo, P.K. Singh, A. Filippov, Colloid J. **76**(6), 725–738 (2014)
37. P.K. Yadav, S. Deo, S.P. Singh, A. Filippov, Colloid J. **79**(1), 160–171 (2017)
38. S.M. Fatemi, H. Sepehrian, M. Arabieh, Europ. Phys. J. Plus **131**(5), 131 (2016)
39. S.M. Fatemi, Z. Abbasi, H. Rajabzadeh, S.A. Hashemizadeh, A.N. Deldar, Eur. Phys. J. D **71**(7), 194 (2017)
40. F. Malekian, H. Ghafourian, K. Zare, A.A. Sharif, Y. Zamani, Europ. Phys. J. Plus **134**(5), 212 (2019)
41. M. Rasoulzadeh, K. Fikri, J. Transp. Porous Med. **116**(2), 613–644 (2017)
42. K.P. Chen, Extreme Mech. Lett. **4**, 124–130 (2015)
43. D. Jayalakshmamma, P. Dinesh, M. Sankar, Mapana J. Sci. **10**(2), 11–24 (2011)
44. S. Liu, J.H. Masliyah, Chem. Eng. Commun. **148–150**(1), 653–732 (1996)
45. D.A. Nield, A. Bejan, *Convection in Porous Media 24* (Springer, Cham, 2006)
46. H.J. Keh, Y.C. Cheng, Colloid Polym. Sci. **283**, 627–635 (2005)
47. S.I. Vasin, A.N. Filippov, V.M. Starov, Adv. Coll. Int. Sci. **139**, 83–96 (2008)
48. J.A. Ochoa-Tapia, S. Whitaker, Int. J. Heat Mass Transfer **38**, 2647–2655 (1995)
49. A.V. Kuznetsov, Appl. Sci. Res. **56**, 53–67 (1996)
50. A.V. Kuznetsov, Int. J. Heat Mass Transf. **41**, 2556–2560 (1998)
51. J. Hartmann, F. Lazarus, Matematisk fysiske Meddelels **15**(7), 1–46 (1937)
52. P.K. Yadav, Int. J. Fluid Mech. Res. **47**(2), 1–18 (2020)
53. P.K. Yadav, A. Tiwari, P. Singh, Acta Mech. **229**, 1869–1892 (2018)
54. H. Ramkissoon, Acta Mech. **123**, 227–233 (1997)
55. D.D. Joseph, L.N. Tao, Zamm **44**, 361–364 (1964)
56. P.K. Yadav, S. Deo, M.K. Yadav, A.N. Filippov, Colloid J. **75**, 611–622 (2013)
57. D. Palaniappan, Z. Angew. Math. Phys. **45**, 832–838 (1994)
58. G.G. Stokes, J. Trans. Camb. Philos. Soc. **9**, 8–106 (1851)